Predicting and mitigating the global warming potential of agro-ecosystems

Simon Lehuger, Benoit Gabrielle, Patricia Laville, Matieyiendu Lamboni, Pierre Cellier, Benjamin Loubet

Predicting and mitigating the global warming potential of agro-ecosystems

S. Lehuger[a] [1] , B. Gabrielle[a], P. Laville[a], M. Lamboni[b], P. Cellier[a], B. Loubet[a]

a: Institut National de la Recherche Agronomique, UMR 1091 INRA-AgroParisTech Environnement et Grandes Cultures,78850 Thiverval-Grignon, France
b: Institut National de la Recherche Agronomique, UR 341 INRA Mathématiques et Informatique Appliquées, 78352 Jouy-en-Josas, France

[1]Corresponding author: UMR1091 INRA-AgroParisTech Environnement et Grandes Cultures, 78850 Thiverval-Grignon, France. E-mail: Simon.Lehuger@grignon.inra.fr Fax: (+33) 1 30 81 55 63 Phone: (+33) 1 30 81 55 24

Abstract

Nitrous oxide, carbon dioxide and methane are the main biogenic greenhouse gases (GHG) contributing to the global warming potential (GWP) of agro-ecosystems. Evaluating the impact of agriculture on climate thus requires a capacity to predict the net exchanges of these gases in an systemic approach, as related to environmental conditions and crop management. Here, we used experimental data sets from intensively-monitored cropping systems in Western Europe to calibrate and evaluate the ability of the biophysical crop model CERES-EGC to simulate GHG exchanges at the plot-scale. The experiments involved major crop types (maize-what-barley-rapeseed) on loam and rendzina soils. The model was subsequently extrapolated to predict CO_2 and N_2O fluxes over entire crop rotations. Indirect emissions (IE) arising from the production of agricultural inputs and from use of farm machinery were also added to the final GWP. One experimental site (involving a wheat-maize-barley rotation on a loamy soil) was a net source of GHG with a GWP of 670 kg CO_2-C eq ha^{-1} yr^{-1}, of which half were due to IE and half to direct N_2O emissions. The other site (involving a rapeseed-wheat-barley rotation on a rendzina) was a net sink of GHG for -650 kg CO_2C eq ha^{-1} yr^{-1}, mainly due to a higher predicted C sequestration potential and C return from crops. Some mitigation options were tested to design productive agro-ecosystems with low global warming impact.

Keywords

Global warming potential; Agro-ecosystem model; CERES-EGC; Bayesian calibration; Greenhouse gases; Nitrous oxide

1 Introduction

While the security of food supply to an increasing population has turned into a pressing issue worldwide, the growing environmental footprint of agriculture due to land use change and management intensification is posing an unprecedented challenge. Assessing the contribution of agriculture to climate change is one of the key questions that environmental scientists have to address in order to identify possible measures to reduce the burden of agriculture on global warming (Sutton et al., 2007; Galloway et al., 2008). Agriculture significantly contribute to anthropogenic greenhouse gas (GHG) emissions with a global flux of 6.1 Gt CO_2-eq yr^{-1} which represent 10-12% of the total GHG anthropogenic emissions (Smith et al., 2007). In the case of arable crops, these emissions include the exchanges of GHG in the cultivated field but exclude the upstream (indirect) emissions.

The direct emissions of GHG by agro-ecosystems are made up of three terms: emissions of nitrous oxide, net carbon fluxes between soil-plant system and the atmosphere, and methane exchanges. Nitrous oxide (N_2O) is produced by soil micro-organisms via the processes of nitrification and denitrification (Hutchinson and Davidson, 1993). Arable soils are responsible for 60% of the global anthropogenic emissions of N_2O (Smith et al., 2007), and their source strength primarily depends on the fertilizer N inputs necessary for crop production. Other environmental factors regulate these emissions: soil temperature, soil moisture, soil NO_3^- and NH_4^+ concentrations, and the availability of organic C substrate to micro-organisms (Conrad, 1996). The effect of these factors results in a large spatial and temporal variability of N_2O emissions (Kaiser and Ruser, 2000; Jungkunst et al., 2006). The second term in the GHG balance, the net C exchanges, is taken as the variations of ecosystem C stock. These variations reflect the balance between C inputs to the agro-ecosystems, via crop residue return, root deposition and organic amendments, and outputs via harvested biomass and soil organic matter mineralization. This term may be

assessed either from long term C stock evolution or, at the rotation scale, by computing the C balance between net carbon exchanges between the soil-plant system and the atmosphere, minus the harvested biomass removed out of the field plus the import of organic C from manure application (Grant et al., 2007; Ammann et al., 2007). Lastly, non-flooded cropland are usually considered as a weak methane-sink that mitigates the global warming potential (GWP) of cropping systems by 1% to 3% (Robertson et al., 2000; Mosier et al., 2005).

Indirect emissions of GHG arising from the production of agricultural inputs (fertilizers, pesticides and lime), fuel combustion and use of machinery on the farm may contribute as much as half of the total GHG budget of agricultural crops (Robertson et al., 2000; Mosier et al., 2005; Adviento-Borbe et al., 2007). Thus, this term provides good leverage to mitigate their impact on global warming (West and Marland, 2002).

The global GHG balance may be expressed as the global warming potential (GWP) of an agro-ecosystem considered, in CO_2 equivalents, using the GWPs of all the trace gases with radiative forcing (IPCC, 2007). Various agricultural practices impact the GHG balance of agro-ecosystems. Some of them may first enhance the carbon sink-strength of soils: conversion to no-tillage practices, the introduction of catch crops, and the incorporation of crop residues into the topsoil were shown to lead to possible C sequestration into the organic carbon pool of the agricultural soils (Smith et al., 2001; Arrouays et al., 2002). The evaluation of candidate agricultural practices to reduce the GWP of agro-ecosystems should encompass indirect and direct emissions of all GHG, to avoid trade-off effects. For instance, because the C and N biogeochemical cycles are interconnected, CH_4 and N_2O emissions may offset the beneficial C storage associated with practices targeting at C sequestration (Six et al., 2004; Desjardins et al., 2005; Li et al., 2005a).

The different crops occurring within a given rotation are inter-related in terms of nutrients' turnover, and soil organic and mineral status. In addition, the nutrients derived from fertilizers or

biological fixation may be recycled or stored into the pools of the SOM, and may be re-emitted into air or water in subsequent years (Del Grosso et al., 2005; Anthoni et al., 2004). That is the reason why it is not relevant to calculate the GWP of a single crop, but rather of a complete sequence of crops. The GWP of this rotation may subsequently be re-allocated to a particular crop based on its frequency of occurrence in the rotation, or similar rules.

In the literature, the GWP of agro-ecosystems is either calculated to assess the effect of the conversion to a new management practice (e.g., no-till, catch crops, farmyard manure application, or land use change; (Robertson et al., 2000; Bhatia et al., 2005; Mosier et al., 2005), or for inclusion into the life cycle assessment of a crop-derived product. These include biofuels, animal feed, or human food (Kim and Dale, 2005; Gabrielle and Gagnaire, 2008; Adler et al., 2007). Direct GHG emissions may be either estimated from direct field measurements (Robertson et al., 2000; Bhatia et al., 2005; Mosier et al., 2005; Adviento-Borbe et al., 2007), or by using biogeochemical models simulating GHG emissions (Del Grosso et al., 2005; Desjardins et al., 2005; Pathak et al., 2005; Adler et al., 2007). Most agro-ecosystems have a positive net GWP (meaning they enhance global warming), but this trend is mainly controlled by the C storage potential of the soil. In the US Midwest, Robertson et al. (2000) measured the GWP of an annual crop rotation (maize-soybean-wheat) as 40 and 310 kg CO_2-C eq ha^{-1} yr^{-1} for no-till and conventional tillage systems, respectively. In Colorado, for rainfed crops under no-till practices, Mosier et al. (2005) measured a topsoil C-storage of about 300 kg CO_2-C eq ha^{-1} yr^{-1} in perennial, rainfed crops under no-till, which offset the other terms in the GHG balance and resulted in a negative net GWP of -85 kg CO_2-C eq ha^{-1} yr^{-1}. Adviento-Borbe et al. (2007) quantified GWPs in four high-yielding maize systems in Nebraska (USA) for continuous maize system and maize-soybean rotations, with recommended and intensive management for both systems. The authors reported that the N_2O fluxes were similar in the different treatments despite the large differences in crop management and N fertilizer applications. As a result, all the systems were net sources

of GHGs with GWPs between 540 and 1020 kg CO_2-C eq ha^{-1} yr^{-1}. Grace et al. (1993) reported GWPs of tropical rice-wheat-cowpea systems in India. In these systems, the net GWP was an order of magnitude higher than GWP from temperate region and ranged between 2400-3200 kg CO_2-C eq ha^{-1} yr^{-1} for no-till and conventional treatments. Three factors explained the difference between temperate and tropical systems: the high soil C loss, the CH_4 emissions from rice cultivation and higher N_2O fluxes (Robertson and Grace, 2004).

The various terms of the net GWP should be predicted with similar accuracy. Indirect emissions may be easily calculated thanks to databases of life cycle inventories (West and Marland, 2002; Nemecek et al., 2003), but direct field emissions of N_2O and C storage in soil are extremely dependant of pedoclimatic conditions and agricultural management practices. To take into account these sources of variability, and to devise mitigation strategies, the processes occurring in the soil-crop-atmosphere system should be modelled simultaneously, together with the effect of agricultural practices. In the past, modelling approaches were developed in parallel either by agronomists seeking to predict crop growth and yields in relation to their management (Boote et al., 1996), or by ecologists focusing on biogeochemical cycles and in particular mineralization, nitrification and denitrification in soils (eg, Li et al. (1992)). With the increasing interest for the prediction of trace gas emissions from arable soils (or pollutants in general), both approaches should be linked together in a more systemic perspective (Gijsman et al., 2002; Zhang et al., 2002). The CERES-EGC model was designed following this philosophy to estimate site-and-management specific environmental balance, or regionalised inventories of trace gas emissions (Gabrielle et al., 2006).

The objectives of this work were: i/ to test and calibrate the CERES-EGC crop model with experimental data from cropping systems representative of northern Europe, ii/ to apply the model to assess the GWP of the cropping systems, including direct and indirect emissions of GHG and iii/ to assess the sensitivity of GWPs to different agricultural practices to purpose options for

mitigation.

2 Material and Methods

2.1 Experimental data

2.1.1 Field sites

The field experiments were carried out at three locations in northern Europe, at Rafidin (northern France, 48.5 N, 2.15 E) in the Champagne region in 1994-1995 (Gosse et al., 1999), at Grignon near the city of Paris (northern France, 48.9 N, 1.95 E) in 2004-2008 and at Gebesee (20 km NW of Erfurt in Germany, 51.1 N, 10.9 E) in 2006-2007.

In Rafidin, the soil was a grey rendzina overlying a subsoil of mixed compact and cryoturbed chalk. The topsoil (0-30 cm) has a clay loam texture, with (31% clay and 28% sand, an organic matter content of 19.5 g kg^{-1}, a pH (water) of 8.3, and a bulk density of 1.23 g cm^{-3}. In Grignon, the soil was a silt loam with 18.9% clay and 71.3% silt in the topsoil. In the top 15 cm, organic carbon content was 20.0 g kg^{-1}, the pH (water) was 7.6 and the bulk density 1.30 g cm^{-3}. In Gebesee, the soil was a Chernozerm (silty clay loam) with 35.8% clay and 60.3% silt in the top 20 cm, organic carbon was 23.0 g kg^{-1}, the pH (water) was 6.7 and the bulk density 1.3 g cm^{-3}. The Table 3 recapitulates the crop sequences of the experimental sites and the main cropping operations. The Rafidin site involved a rapeseed - winter wheat - winter barley rotation, and the measurements essentially took place during the rapeseed growing cycle, from its sowing on 9 Sept., 1994 to its harvest on 11 July, 1995. Three fertilizer N treatments (N0=0 kg N ha^{-1}, N1=135 kg N ha^{-1} and N2=270 kg N ha^{-1}) were established on 30×30 m blocks arranged in a split-plot design with three replicates. For this site, the rotations we simulated were only different regarding the fertilizer N inputs on the rapeseed crop. The other crops in the rotation (wheat and barley) were managed identically in the N0, N1 and N2 rotations.

At the Grignon site, two experiments were monitored in parallel on two fields: a principal field

(Grignon-PP, 19 ha), on which a maize - winter wheat - winter barley - mustard rotation was monitored since 2004 and 3 adjacent plots (Grignon-PAN1, -PAN2, -PAN3, 2500 m^{-2} each) on another field on which the same rotation was applied since 2006, with 0, 1 and 2 years time-lag interval in order to have all the crops each year. The adjacent plots were monitored since 2006. In the rotation, a mustard was planted following the harvest of barley the year before to serve as a catch crop to reduce nitrate leaching. On the principal field, dairy cow slurry was applied between the harvest of barley and the planting of mustard on 31 August 2004, and before the maize sowing on 16 April 2008.

In Gebesee, the crop sequence from 2003 to 2007 was rapeseed - winter barley - sugar beet - winter wheat. Two applications of organic fertilizers were carried out in 2007, one application of cattle slurry (18 m^3 ha^{-1}) on the wheat crop in 11 Apr. and 35 t ha^{-1} of farmyard manure in 4 Sept after harvest.

2.1.2 Soil and crop measurements

Soil mineral nitrogen content (NO_3^- and NH_4^+) and moisture content were monitored in the following layers: 0-15 cm, 15-30 cm, 30-60 cm and 60-90 cm at Grignon, 0-30 cm, 30-60 cm, 60-90 cm, and 90-120 cm at Rafidin, and 0-10 cm and 10-20 cm at Gebesee. Soil samples were taken in triplicates with an automatic (Rafidin) or manual (Grignon and Gebesee) auger every 1 to 4 weeks, and analysed for moisture content and mineral N. The latter involved an extraction of soil samples with 1 M KCl and colorimetric analysis of the supernatant. In the three sites, soil moisture and temperature were also continuously recorded using TDR (Time Domain Reflectrometry, Campbell Scientific, Logan, Utah, USA) and thermocouples. Soil bulk density was measured once in each site, using steel rings. For both experiments of Grignon and Rafidin, plants were collected every 2 to 4 weeks, and separated into leaves, stems, ears or pods, and roots. Leaf area index was measured with an optical leaf area meter or analysis of leaf scans.

The plant samples were dried for 48 h at 80° C and weighted, and analysed for C, N, P and K content by flash combustion.

2.1.3 Trace gas fluxes and micrometeorological measurements

At the three sites, daily climatic data were recorded with an automatic meteorological station, including maximum and minimum daily air temperatures (° C), rainfall (mm day^{-1}, solar radiation (MJ m^{-2} day^{-1}) and wind speed (m s^{-1}). At Grignon and Gebesee, the measurements of CO_2 fluxes at the field scale were carried out in the framework of the CarboEurope integrated project (European Commission Framework VI research programme; Aubinet et al. (2000)). Water vapour and CO_2 fluxes were measured using the eddy covariance method above the crop canopy. Wind speed was monitored with a three-dimensional sonic anemometers, and CO_2 concentration with infrared gas analysers (model Li-7500 in Grignon and model Li-7000 in Gebesee; LiCor Inc., Lincoln, NE, USA) located on a mast at two meters above the canopy. Daily net ecosystem carbon dioxide exchange (g C m^{-2} day^{-1}), and its daily evapotranspiration (mm m^{-2} day^{-1}) were calculated by integrating the 30-minute fluxes determined by the micrometeorological measurements over each day. The eddy covariance technique usually produces gaps in the half-hourly C flux data, making it necessary to fill the missing values before integration at the daily time scale. The gap-filling methodology of CarboEurope-IP was applied to the experimental data sets (Falge et al., 2001).

At Rafidin, there were no micrometeorological measurements of CO_2 exchanges. Nitrous oxide emissions were monitored by the static chamber method using circular chambers (0.2 m^{-2}), with 8 replicates. On each sampling date, the chambers were closed with an airtight lid, and the head space was sampled 4 times over a period of 2 hours. The gas samples were analysed in the laboratory by gas chromatography. The measurements were done every 1-3 weeks between September, 1994 and April, 1995 (Gosse et al., 1999). For the Grignon-PP experiment, N_2O

emissions were measured with 3 to 6 automatic chambers (55 L, 0.5 m^{-2}). The chambers were sequentially closed during 15 min and the complete cycle for the six chambers was then fixed to 1h30. The N_2O concentrations were measured using an infrared gas analyser (N_2O Analyser 46C, Thermo Scientific Inc., Waltham, MA, USA) which was connected on line with the chambers. Air was pumped from the chamber to the gas analyser and injected again after the analysis to the chambers. Nitrous oxide fluxes were calculated from the slope of the gas accumulation rate. The electric jacks used to open and close the chambers and the solenoid valves were controlled by a Campbell data logger (CR23X, Logan, Campbell Scientific, Utah, USA) that recorded the N_2O concentration every 10 seconds. Nitrous oxide emissions were monitored for 442 days from January 1, 2007, to August 31, 2008. During this period, the mean value of the emissions was 8.7 g N_2O-N ha^{-1} d^{-1}. Eight manual chambers were also disposed in the field in order to measure N_2O, CO_2 and CH_4 fluxes on a monthly frequency or following the fertiliser application. A more intensive monitoring of the GHG emissions was carried out following the slurry application in spring 2008.

For the three Grignon-PAN plots, the three GHGs (N_2O, CO_2 and CH_4) were measured with 5 static circular chambers (0.2 m^{-2}) per plot. The chambers were closed over a period of 30 minutes and 4 gas samples were collected with a syringe at 0, 10, 20 and 30 minutes after closure. Gas samples were analysed by gas chromatography fitted with an electron capture detector for N_2O analysis and with a flame ionisation detector and a methaniser for CO_2 and CH_4 analysis. In Gebesee, GHG measurements were carried out with manual chambers ($100 \times 100 \times 30$ cm - when crop is higher than 30cm height was expanded to 60cm) from Feb. 2006 to Dec. 2007, weekly during growing season and every two weeks otherwise. The chambers were closed for one hour and sampling was carried out every 20 minutes during closure. From Feb. to Dec. 2007, two automatic chambers ($95 \times 25 \times 125$ cm) were installed in the same plot. Gas samples were automatically collected every 20 minutes during one hour of closure and each chamber was

closed 6 times in a day. In both cases, gas samples were analysed with gas chromatography such as described above.

At the dates of mineral or organic fertiliser application, the chambers were closed during the spreading operation and then, the amount corresponding to the chamber surface was applied by hand within the chambers.

2.2 The indirect GHG emissions

The GHG emissions (CO_2, N_2O and CH_4) associated with input production and use of farm machinery were calculated from the Ecoinvent life cycle inventory database (Nemecek et al., 2003). The inventory of elementary management operations comprises soil tillage, fertilisation, sowing, plant protection, harvest and transport, and may be translated in terms of GHG emissions thanks to emission factors. Similarly, the production of agricultural inputs (fertilizers, pesticides, seeds and agricultural machinery) induces GHG emissions that arise mainly from fossil fuel combustion, and were included in the indirect emissions.

2.3 Global warming potentials of crop rotations

For arable fields, the carbon balance is calculated as the net biome production (NBP) equal to:

$$NBP = NEP - Exported\,biomass + Imported\,biomass \quad (1)$$

The NEP is the net ecosystem production and corresponds to the net C exchanges between soil-plant system and the atmosphere, above the canopy. The exported biomass is the harvest and the imported biomass may be application of manure or compost. The carbon dioxide exchanges for a crop growing cycle were assumed to start from their sowing to the sowing of the following crop. The sign convention used to express NBP as positive quantity with net carbon fixation, were inverted in the calculation of the GWP. The values of NBP were obtained by averaging the NBP simulated over 12 maize-wheat-barley-mustard rotations on a 36-yr series of historical

weather data (1972-2008) in Grignon-PP, with constant crop management. The same simulation was done for the three treatments of Rafidin over 9 rapeseed-wheat-barley rotations on a 28-yr series of weather data. The 30-yr simulation allowed us to explore the climatic variability and its effect on the net primary production and soil respiration.

The global warming potential of crop sequences was computed by adding NBP, N_2O emissions, CH_4 exchanges and the indirect emissions using global warming potential of the GHGs at the 100-year time horizon (CO_2=1, CH_4=25 and N_2O=298, IPCC (2007)).

2.4 The CERES-EGC model

CERES-EGC was adapted from the CERES suite of soil-crop models (Jones and Kiniry, 1986), with a focus on the simulation of environmental outputs such nitrate leaching, emissions of N_2O ammonia, and nitric oxide (Gabrielle et al., 2006). It can therefore be used as an agronomic tool to improve the management of major arable crops, based on crop productivity and environmental criteria. The model simulates the cycles of water, carbon and nitrogen within agro-ecosystems (Gabrielle et al., 1995, 2006).

Direct field emissions of CO_2, N_2O, NO and NH_3 into the atmosphere are simulated with different trace gas modules. Here, we focus on gas fluxes with global warming potential, i.e. CO_2 and N_2O.

Carbon dioxide exchanges between soil-plant system and the atmosphere are modelled via the net photosynthesis and SOC mineralization processes. Net primary production (NPP) is simulated by the crop growth module while heterotrophic respiration (Rs) is deduced from the SOC mineralization rates calculated by the microbiological sub-model. The net ecosystem production (NEP), which is calculated as NPP minus Rs, may be computed on a daily basis and directly tested against the net ecosystem exchanges measured by eddy covariance.

CERES-EGC uses the semi-empirical model NOE (Hénault et al., 2005) for simulating the N_2O

production in the soil through both the nitrification and the denitrification pathways. Denitrification component is derived from the NEMIS model (Hénault and Germon, 2000) that calculates the denitrification as the product of a potential rate with three unitless factors related to soil water content, nitrate content and temperature. Nitrification is modelled as a Michaëlis-Menten reaction with NH_4^+ as substrate that additionally is controlled by response functions of the soil water content and temperature. Nitrous oxide emissions resulting from the two processes are soil-specific proportions of total denitrification and nitrification pathways.

CERES-EGC runs on a daily time step and requires input data for agricultural management practices, climatic variables (mean air temperature, daily rain and Penman potential evapotranspiration), and soil properties.

2.5 Parameter selection and model calibration

Dynamic biophysical models include a large number of parameters whose values are uncertain and it is often impossible to estimate all these parameters accurately and simultaneously. A common practice consists in selecting a subset of parameters by global sensitivity analysis, then estimating the selected parameters against experimental data and setting the others to nominal values (Makowski et al., 2006). In our case, a multivariate global sensitivity analysis, developed by Lamboni et al. (2009), allowed us to select the 6 most sensitive parameters of the N_2O emission module of CERES-EGC. The most influent parameters were then estimated with a Bayesian calibration approach. Table 1 recapitulates the parameters involved in the calibration. The calibration was applied with the N_2O emission measurements of the experimental site of Grignon-PP and the calibrated parameters were then used to simulate the fields of Grignon-PAN and Gebesee experiments. The parameters values used for the Rafidin site originated from a previous calibration (Lehuger et al., 2009).

Van Oijen et al. (2005) and Lehuger et al. (2009) described in details the Bayesian method that

was used in this work. Briefly, the aim of Bayesian calibration is to reduce the prior parameter uncertainty by using measured data, thereby producing the posterior distribution for the parameters. In our case, we specified lower and upper bounds of the parameters uncertainty, defining the prior parameter distributions as uniform (Table 1). Posterior pdf is then computed by multiplying the prior with the likelihood function, which is the probability of the data given the parameters. Because probability densities may be very small numbers, rounding errors needed to be avoided and all calculations were carried out using logarithms. The logarithm of the data likelihood is thus set up, for each data set Y_i, as follows:

$$logL_i = \sum_{j=1}^{K} \left(-0.5 \left(\frac{y_j - f(\omega_i; \theta_i)}{\sigma_j} \right)^2 - 0.5log(2\pi) - log(\sigma_j) \right) \quad (2)$$

where y_j is the mean N_2O flux measured on sampling date j in the data set Y_i and σ_j the standard deviation across the replicates on that date, ω_i is the vector of model input data for the same date, $f(\omega_i; \theta_i)$ is the model simulation of y_j with the parameter vector θ_i, and K is the total number of observation dates in the data sets. To generate a representative sample of parameter vectors from the posterior distribution, we used a Markov Chain Monte Carlo (MCMC) method: the Metropolis-Hastings algorithm (Metropolis et al., 1953). For each calibration, three parallel Markov chains were started from three different starting points in the parameter space (θ_0). Convergence was checked with the diagnostic proposed by Gelman and Rubin (1992). The chains were considered to be a representative sample from the posterior pdf, and from this sample were calculated the mean vector, the variance matrix and the 90% confident interval for each parameter.

Parameter vector $\theta = [\theta_1 ... \theta_6]$					Prior probability distribution		Posterior probability distribution		
θ_i	Symbol	Description	Unit	Default value	θ_{min}(i)	θ_{max}(i)	Mean	SD	Correlated $\{\theta_i\}$
θ_1	r	Ratio of N_2O to total denitrification	%	0.09	0.20	0.90	0.36	0.09	{2,4,5,6}
θ_2	PDR	Potential denitrification rate	kg N ha^{-1} d^{-1}	0.1	6.0	20.0	0.33	0.61	{2,1,5,6}
θ_3	Tr_{WFPS}	WFPS threshold for denitrification	%	0.62	0.40	0.80	0.61	0.05	{2,4,5}
θ_4	POW_{denit}	Exponent of power function	Unitless	1.74	0.00	2.00	0.46	0.21	{1, 3}
θ_5	Km_{denit}	Half-saturation constant (denit)	mg N kg^{-1} soil	22.00	5.00	120.00	24.69	17.53	{1,2,3,6}
θ_6	TTr_{denit}	Temperature threshold	°C	11.00	10.00	15.00	10.05	0.17	{1,2,5}

Table 1: Description of the 6 selected parameters of the N_2O emissions module. The prior probability distribution is defined as multivariate uniform between bounds θ_{min} and θ_{max}. The posterior parameter distributions are based on the calibration with the Grignon-PP data set, and are characterised by the mean value of the posterior, their standard deviation (SD). Correlations with other parameters are reported if their absolute value exceeds 0.4 (underlined parameters express a negative correlation).

2.6 Model evaluation

Two statistical indicators were used to evaluate the performance of the model to fit with the observed data. Mean deviation (MD) was defined as:

$$MD = \frac{1}{K}\sum_{j=1}^{K}(y_j - f(\omega_k;\theta_l)) \tag{3}$$

and the root-mean squared error (RMSE) as:

$$RMSE = \sqrt{\frac{1}{K}\sum_{j=1}^{K}(y_j - f(\omega_k;\theta_l))^2} \tag{4}$$

where y_j is the time series of the observed data on day j of data set D_i, and f($\omega_k;\theta_l$) is the corresponding model predictions with input variables ω_k and parameters θ_l.

The RMSE was computed for the experiments used in the calibration (Grignon-PP and Rafidin) and in the subsequent model testing against the independent data sets of Grignon-PANs, and Gebesee. In both last cases, the RMSE corresponds to the root mean square error of prediction (RMSEP(θ)), since the data were involved neither in parameter estimation nor model development (Wallach, 2006). The RMSEP was computed for the predictions of N_2O emissions.

2.7 Scenarios of mitigation

Five scenarios of mitigation were tested in order to assess the effect of agricultural practices on the GWP, and to explore the potential of GHG abatement for crop systems. The scenarios were tested on the Grignon-PP rotation simulated on a 30 year time period. The first scenario ("Straw") was designed to asses the effect of non removing straw out of the field. The scenario ("Catch crop") was designed to assess the effect of catch crop in the rotation by comparing rotations with and without catch crop, which was mustard between a winter crop and a spring crop in our case. We also tested the effect of N fertilisation on the GWP by simulating rotations with 50% less N fertiliser application (scenario "N-") or with with 50% more (scenario "N+"). The last scenario

("Organic") was run to evaluate the effect of C and N input from slurry application every three years on the GWP of the rotation.

3 Results and discussion

3.1 Model testing

3.1.1 Crop growth

At Grignon, the crop growth was well simulated for the various crop species of the rotation, as reported in Fig. 1. The time course of total above ground biomass was correctly captured by the model with the exception of the 2008 maize upon harvest whose dry matter was under-estimated. The maize silage yields were under-estimated in 2005 and 2008 with bias (observed - simulated yields) of 1960 and 6740 kg DM ha^{-1}, respectively, due to too high water stress simulated. Grain yields of barley and winter wheat were correctly predicted and the bias between simulations and observations were -100 and -430 kg DM ha^{-1}

At the Rafidin site, CERES-EGC provided good simulations of rapeseed growth for the N1 and N2 treatments (Fig. 2). The simulated patterns of biomass, LAI and N content variations matched the observations over the entire growing cycle. Final grain yields were correctly estimated, with a simulated value of 3.8 t DM ha^{-1} and an observed one of 4.1 t DM ha^{-1} for N1, and an exact match at 4.9 t DM ha^{-1} for N2. For the N0 treatment (unfertilized), the model overestimated LAI by a factor of 2 throughout the growing season, but total above ground biomass was underestimated by about 25% when compared to the data (not shown). For this treatment, the simulated N stress was too high at the end of the crop's growing cycle to allow sufficient grain filling, and the final grain yield was under-estimated as a result.

3.1.2 Net carbon exchanges

The carbon dioxide exchanges measured with micrometeorological systems were used to calibrate the CERES-EGC model against net ecosystems exchange measurements and to evaluate the model prediction accuracy with independent data (Lehuger et al., 2009). The measurements from Grignon-PP were used for the parameter estimation and those of Gebesee for evaluation of the model prediction accuracy. For both sites, NEP was well simulated at daily and seasonal scales (Fig. 1 and Fig. 3). The RMSE computed for the Grignon-PP experiment was 1.90 g C $m^{-2}d^{-1}$ (n=1627) and the RMSEP of Gebesee 1.5 g C $m^{-2}d^{-1}$ (n=310).

3.1.3 Soil drivers of N_2O emissions

Figure 4 provides a test for the simulation of the key drivers of N_2O emissions at the Grignon-PP site. Soil moisture, temperature and inorganic N content control N_2O emissions by their influence on the nitrification and denitrification processes. At Grignon, for the period of measurement (2006-2008), their dynamics were well simulated (Fig. 4.a, 4.b, 4.c). Table 2 recapitulates the mean deviations (MD) and RMSEs computed with the different soil drivers used as input variables of the N_2O emission module. Soil temperature and soil water content were well predicted by the model with RMSE close to 3°C for the soil temperature and from 4 to 8% (v/v) for the soil water content across the field-site experiments. The model's RMSE over the 8 experiments ranged between 9.9 and 57.0 kg N ha^{-1} for the simulation of nitrate content and to 4.1 to 28.6 kg N ha^{-1} for the ammonium content. The model did not captured the N dynamic in the Grignon-PAN2 field site due to a lack of correlation between N content and N fertiliser applications in this plot.

Site	Treatment	Soil temperature				Soil water content				Nitrate content				Ammonium content			
		N	Mean	MD	RMSE	N	Mean	MD	RMSE	N	Mean	MD	RMSE	N	Mean	MD	RMSE
			(°C)				(v/v)				(kg NO_3-N ha^{-1})				(kg NH_4-N ha^{-1})		
GRIGNON	PP	637	10.9	-1.1	3.0	492	0.318	0.016	0.033	24	49.4	23.2	40.7	24	10.6	7.2	11.0
	PAN1	-	-	-	-	14	0.238	-0.039	0.064	13	36.7	-2.3	21.6	13	10.1	6.8	12.5
	PAN2	-	-	-	-	17	0.238	-0.045	0.064	16	71.9	31.2	57.0	16	17.8	14.2	23.5
	PAN3	-	-	-	-	15	0.255	-0.029	0.042	14	26.5	-3.8	22.7	14	6.1	3.4	4.9
GEBESEE		729	10.7	-0.2	3.3	649	0.260	-0.065	0.080	78	18.1	-1.1	24.5	78	7.7	4.4	28.6
RAFIDIN	N0	294	8.7	-1.2	3.0	20	0.253	-0.027	0.043	21	10.8	5.5	9.9	21	3.7	3.5	4.1
	N1	294	8.7	-1.2	3.0	20	0.244	-0.035	0.051	21	12.9	8.0	11.8	21	5.6	5.0	6.8
	N2	294	8.7	-1.2	3.0	20	0.240	-0.039	0.050	21	23.5	17.0	22.6	21	6.2	5.6	8.0

Table 2: Sample size (N), mean of measured in situ soil variables (Mean), mean deviation (MD) and root mean square errors (RMSE) computed with the predicted and measured soil variables: soil temperature, soil water content and topsoil nitrate and ammonium contents for the 8 data sets.

3.2 Nitrous oxide emissions

The three parallel chains ran for the Bayesian calibration against Grignon-PP site, converged well for all the parameters after 50 000 iterations. The Table 1 summarizes the posterior expectancy of parameters and their standard deviation. Correlations with other parameters are also reported in Table 1. The posterior ratio of N_2O to total denitrification was higher than is default value, while the posterior potential denitrification rate was highly reduced in comparison with its default values, 0.33 vs. 6.00 kg N ha^{-1} d^{-1} respectively. The posterior value of WFPS threshold for denitrification, the half-saturation constant for denitrification and the temperature threshold were similar of their default values.

The Fig. 5 compares the simulations of daily N_2O emissions after calibration and the observations of the Grignon-PP experiment. There was good agreement between simulated and observed data during the mineralization of crop residues of the barley at the end of 2007 and beginning of 2008. The first peak flux in March 2007, corresponding to the first N fertiliser application, was not captured by the model due to WFPS simulated above 61% - the threshold that triggers denitrification in the model. The high peak fluxes that occurred in spring 2008 consecutive to the slurry and N-fertiliser applications for maize were correctly predicted. The N_2O emissions observed during the time period consecutive to theses peaks were low and the model simulated emissions close to zero. The RMSE obtained with the posterior expectancy of parameters was reduced by 30% in comparison with the default parameter values (Table 4).

The Fig. 6 shows the dynamic of N_2O emissions for the three treatments of the Rafidin sites. At this site, N_2O emissions were very low even for the high-N input treatment (N2). In fact, for this treatment, the highest emission rate measured was 7.4 g N_2O-N ha^{-1} d^{-1}. In this site, the rates of N_2O emissions from denitrification were close to zero. Hénault et al. (2005) estimated that 98% of the N_2O emissions originated from the nitrification process at the same Rafidin site. The predicted rates of N_2O emissions were satisfactory, with RMSEs of 0.3, 1.4 and 3.0 g N_2O-

N ha^{-1} d^{-1} after calibration for the N0, N1 and N2 treatments respectively (Table 4).

The calibrated model was used to simulate the experiments of Grignon-PAN1,-PAN2 and -PAN3 and of Gebesee. By this way, we assessed the model prediction accuracy by computing the RMSEP, reported in Table 4. The predictions computed with the calibrated parameter set were improved in comparison with the predictions with default parameters values, by 6.3% in average for the Grignon-PAN1, -PAN2, -PAN3 treatments and by 39% for Gebesee experiment. The Fig. 7 depicts the N_2O emissions over one year for the three treatments PAN1, PAN2 and PAN3 of the Grignon site and shows that the model correctly predicts the N_2O emission peaks consecutive to the N-fertiliser application that occurred in spring 2008, and also the period of low emissions. The Fig. 8 shows the time course of N_2O emissions at Gebesee. The low emissions and most of the N_2O peaks were well simulated by the model. However, the model can not predict the N_2O deposition and N_2O emissions due to freeze-thaw cycles in winter.

3.3 Simulation of crop rotations

In the previous section, we tested and calibrated the CERES-EGC model against datasets from 8 field site experiments involving different sets of crop types, pedoclimatic conditions, and agricultural practices. The present section deals with the extrapolation of the model to calculate the GWP of complete cropping systems, including net C exchanges, direct emissions of N_2O and CH_4 fluxes in the field. The last term of the GHG balance, namely the indirect emissions, was also added.

3.3.1 Net biome production

Fig. 9 displays the breakdown of the NBP for the Grignon-PP rotation. The net ecosystem production was highest with the maize crop, amounting to 5830 $\pm$ 690 kg C ha^{-1}, whereas the NEP of the wheat was 5300$\pm$750 and those of barley close to 4800$\pm$630 kg C ha^{-1}. For the mustard, the soil respiration term was greater than net photosynthesis, and NEP was -440 kg C ha^{-1}. In

Rafidin, the NEP of rapeseed was 1300 ± 1420, 4260 ± 995 and 4640 ± 1170 kg C ha^{-1} for the N0, N1 and N2 treatments, respectively, the NEP of wheat was between 4870 and 5190 and the NEP of barley between 3150 and 3440 kg C ha^{-1}. Inter-annual variability was quite large for the net primary production, showing a strong dependence of the climate on crop growth.

Over long-term simulation period with the maize-wheat-barley-mustard rotation in Grignon-PP, we estimated a stable C stock with 10 kg C ha^{-1} yr^{-1} sequestered on average. In Rafidin, we estimated large C accumulation of 525, 1153 and 1269 kg C ha^{1} yr^{-1} for the N0, N1 and N2 treatments, resp., due to a minor part of the fixed C which was exported out of the field. In Grignon, the straw of wheat and barley was removed for use as litter for animal production, whereas in Rafidin the straw was left on the soil surface at harvest, and subsequently incorporated into the topsoil layer. As a consequence, the C inputs from crop residues were much higher in Rafidin than in Grignon, averaging 4250 kg C ha^{-1} yr^{-1}for the N1 rotation and 4290 kg C ha^{-1} yr^{-1}for the N2 rotation. With these levels of C inputs to the soil, the CERES-EGC model predicted a high C sequestration for the rotations of Rafidin suggesting that the Rafidin soil was a potentially large sink for atmospheric CO_2.

For the other experimental fields of Grignon, the NBPs were 85 for the PAN1 treatment, -256 for the PAN2 treatment and -32 kg C ha^{-1} yr^{-1} for the PAN3 treatment.

3.3.2 Indirect emissions

The GHG cost of agricultural inputs contributes a large part of the GWP of agro-ecosystems. For the Grignon-PP cropping system, the mean indirect emissions were 350 kg CO_2-C eq ha^{-1} yr^{-1}, for the Rafidin system, the mean IE were 320, 410 and 460 kg CO_2-C eq ha^{-1} yr^{-1} for the N0, N1 and N2 treatments, respectively. For the Grignon-PAN treatments, the mean IE were 420, 480 and 410 kg CO_2-C eq ha^{-1} yr^{-1} for PAN1, PAN2, PAN3 treatments. The IE were 590 kg CO_2-C eq ha^{-1} yr^{-1} for the wheat crop cycle of Gebesee, a higher value compared to the other site

due to more frequent cropping operations. N fertilizer production is the top contributor to the IE by a wide margin, with a 55-75% share (Fig. 10). Cropping operations came next, with a 30-40% in the total IE term, mainly due to from fossil-fuel combustion by farm machinery. The transport of inputs from the production plant to the farm was the lowest contributor to the GWP with less than 1% of IE.

3.4 Global Warming Potential

The 30-yr simulation period enabled us to explore the effect of climate variability on biomass production and N_2O emissions. At Grignon-PP, N_2O emissions averaged 316$\pm$ 82 kg CO_2-C eq ha^{-1} yr^{-1} (CV=26%) over maize-wheat-barley-mustard rotation, and we estimated a GWP of 670$\pm$150 kg CO_2-C eq ha^{-1} yr^{-1} (Table 5) for this system. Methane measurements from manual chambers allowed us to estimate its contribution to the final GWP. The soil of Grignon was a weak methane sink that mitigated the GWP of the rotation by 2%. However, the slurry application during mustard cropping cycle induced a large methane emission of 660 g CH_4-C d^{-1} the day of application.

At Rafidin, we estimated three times lower N_2O emissions than in Grignon-PP ($<$140 kg CO_2-C eq ha^{-1} yr^{-1}), and a large C storage potential resulting from the high level of residue return. The more than offset the emissions of N_2O and the indirect emissions, so that the GWP were -90$\pm$150, -621$\pm$135 and -673$\pm$139 kg CO_2C eq ha^{-1} yr^{-1} for the N0, N1 and N2 systems, respectively (Table 5). The Rafidin crop rotation is an intensive system with a high level of inputs and indirect emissions of GHG, but it is compensated for by the resulting high potential of biomass production and SOC storage. Overall, the Rafidin system emerges a potentially strong sink of GHG.

The Table 6 summarizes the GWP for the PAN1, PAN2, PAN3 treatments of Grignon and that of the wheat crop cycle of Gebesee. For each field site, only one crop sequence was simu-

lated. The Grignon-PANs experiments had the same crop sequences as Grignon-PP but without slurry application and maize was harvested for grain and not for silage as it was the case in Grignon-PP. The PAN1, PAN2 and PAN3 treatments were net sources of GHGs with 509, 913 and 547 kg CO_2C eq ha^{-1} yr^{-1}, resp. The net GWP was higher in the PAN2 treatment due to an additional N fertiliser application on wheat in comparison with the two other treatments. In Gebesee, the wheat crop was a high sink of GHGs due to high C input from manure and slurry applications during its cropping cycle.

3.5 Mitigation strategies

Figure 11 compares the GWP of five scenarios with differentiated management crop practices. The initial scenario was the cropping system of Grignon-PP described in section 2.7 and the sensitivity of its GWP was assessed by changing management of crop residues, catch crop in the rotation, N mineral fertiliser amount and CN inputs from organic fertiliser application. The scenario SW with straw not removed out of the field presents the lowest GWP due to a high negative CO_2 balance. Despite of a substantial increase of soil respiration (+50% compared to the initial scenario), the return of C from crop residues makes the soil C stock increased by 265 kg C ha^{-1} yr^{-1} that offsets the other GHG emissions and makes the GWP 35% less emitter of GHGs than the initial scenario (434 kg CO_2-C ha^{-1} yr^{-1}).

The effect of catch crop was assessed by running simulations without sowing mustard between barley and maize. The effect on the GWP was minor (+6% compared to the initial scenario) due to a very low C fixation simulated in the initial scenario and the C input from slurry application that made mustard a strong C sink was displaced on the barley crop.

The N fertilisation affects the GWP due to its effects on fixation, N_2O emissions and indirect emissions. Increasing the amount of mineral N fertilisers by 50% involved a GWP 22% higher than that of the initial scenario for which the N fertilisation was balanced in relation to N crop

demand. N_2O emissions were increased by 17%, indirect emissions by 27% and net primary production only by 1% meaning that optimal yield was already reached with fertilisation of initial scenario. On the contrary, decreasing the N fertiliser by 50% led to a 27% decrease of GWP compared to initial scenario.

We assessed in the last scenario, the effect of slurry application on the GWP. Organic fertiliser application represent large C and N inputs in the crop system and its elimination of the rotation resulted in a three-times higher GWP in comparison with initial scenario. Slurry brought in the crop system 1760 kg C ha^{-1} yr^{-1} which represented half of the C removed by straw removal.

4 Discussion

4.1 Relevance of modelling to estimate GHG balances

The first objective of this work was to test and calibrate the CERES-EGC model against experimental data of CO_2, N_2O, soil variables and crop biomass, from 3 temperate sites located in Western Europe. The model well captured the time course of total above-ground biomass for the crops of the rotations (maize, wheat, barley, rapeseed). The net carbon exchanges between the soil-plant system and the atmosphere were in agreement with the measurements from daily time scale to cropping cycle season and rotations. For the 8 experimental sites and treatments, the soils drivers for N_2O emissions were correctly reproduced and, accordingly, N_2O emissions were in agreement with the observations in all sites with RMSEs or RMSEPs ranging from 0.3 to 14.2 g N_2O-N ha^{-1} d^{-1}. Bayesian calibration applied on the six most influent parameters of the nitrous oxide emission module of CERES-EGC allowed us to reduce error of prediction by 6-40% compared to default parameters-based simulations against 4 independent data sets of N_2O measurements.

Other studies with similar modelling approaches mention that the discrepancies between modelled and observed N_2O data were in the same range of errors as our simulations. For exam-

ple, Del Grosso et al. (2005) showed that the DAYCENT model gave daily prediction of N_2O emissions with a quite high discrepancy (RRMSE=64%, n=21) for major crops in the USA. Del Grosso et al. (2008) also reported that DAYCENT largely overestimated N_2O emissions in irrigated system due to an over responsive effect of soil NO_3^- on N_2O. In the same way, Babu et al. (2006) indicate that the DNDC model predicted daily N_2O fluxes with a large lack of fit (RMSE=529.6 g N_2O-N ha^{-1} d^{-1}, n=134) for rice-based production systems in India with high level of N_2O emissions (observed daily mean=49.4 g N_2O-N ha^{-1} d^{-1}). Frolking et al. (1998) and Li et al. (2005b) compared different models or sub-models for their capacity to simulate N_2O emissions from cropland. In most cases, the models were not able to capture the daily N_2O flux patterns because of time lag between observed and modelled peaks and over- or underestimation of the measured N_2O spikes.

Regarding the C balance, we assumed that the net biome production reflected the SOC changes. The balance between C inputs and C losses of the Grignon-PP field-site was nearly balanced, while Rafidin had a high potential of C sequestration resulting from a high C fixation by crops and a large fraction of inputs as crop residues. As a consequence, C storage was estimated between 500 and 1300 kg C ha^{-1} yr^{-1} for the various treatments of Rafidin. This is in agreement with the relatively low SOC mineralization rate of rendzina soils ($<$0.5% of SOC yr^{-1}), such as that of Rafidin, due to physical protection process by the formation of calcite formation on the organic fractions (Trinsoutrot et al., 2000). The high level of biomass production made possible by ample fertilizer inputs, together with this low SOC mineralization rate induced a large net fixation of atmospheric CO_2. Adviento-Borbe et al. (2007) measured the SOC changes over a 5-yr period in continuous maize system with recommended and intensive fertilisation treatments (+70-100% more N fertiliser applied than in the recommended treatment) in Nebraska (USA). They reported that C sequestration rates ranging from 440 to 620 kg C ha^{-1} yr^{-1} for recommended and intensive treatments, resp., mainly due to high C residue returns from maize crops.

The latters ranged between 5500 and 6500 kg C ha^{-1} yr^{-1} in both cropping systems. In Rafidin, C storage for the intensive rotation was almost twice greater than those of the intensive treatment reported by Adviento-Borbe et al. (2007) whereas the crop residues were slightly lower.

The C dynamics predicted by the model were evaluated at the daily time scale against micrometeorological measurements of CO_2 exchanges for entire crop rotations, but it will be necessary to supplement this test by further verifying the ability of CERES-EGC to simulate the rate of soil C changes in the long term. With this test, we could also compare the methods of estimation of C term by computing either NBP or long-term simulations for assessing change of soil C stock.

4.2 Model application for predicting global warming potential

Applying the model to predict the GWPs of crop rotations was the second objective of this work. Climate variability on the different terms of the GHG balance was taken into consideration by computing the direct emissions over $\sim$30-yr time series as the succession of $\sim$10 rotations. As a result, the GWPs of Rafidin and Grignon-PP were markedly different: the rapeseed-wheat-barley rotation on a rendzina was a net sink of GHG with a GWP of -620 to -670 kg C ha^{-1} yr^{-1} for balanced and intensive treatments, while the wheat-maize-barley-mustard rotation on a loamy soil in Grignon was a net source of GHG, with a GWP of 670 kg C ha^{-1} yr^{-1}.

Few other references of GWP of crop rotations, in particular in Europe were available for comparison with our results. The GWP of Grignon is twice higher than that of 310 kg CO_2-C eq ha^{-1} yr^{-1}, measured by Robertson et al. (2000) for a conventional maize-soybean-wheat system in the US Midwest United States. The latter authors found no measurable soil C sequestration with conventional tillage, and our estimation was also close to zero (-10 kg CO_2-C eq ha^{-1} yr^{-1}). However, their rotation included a legume crop (soybean) that required less N fertilizer amount than cereal or oilseed crops as into our rotation. In addition, the system boundaries they set for the indirect emissions were narrower than ours. They only accounted

for the CO_2 emissions occurring during the production of agricultural inputs, and not the other GHGs, although these may account for half of the total IE of GHG. Consequently, we estimated a twice higher IE term. In both cases, N_2O emissions contributed 50% of the GWP but we estimated a N_2O term twice higher than their estimate from measurements, 316 vs. 142 kg CO_2-C eq ha^{-1} yr^{-1}, respectively. Our estimations of indirect emissions are much more closer of those of Adviento-Borbe et al. (2007) who estimated indirect emissions that ranged between 290 and 660 kg CO_2-C eq ha^{-1} yr^{-1} for continuous maize and soybean-maize cropping systems (without accounting GHG contribution of irrigation and grain drying).

4.3 Efficiency of mitigation options

The last objective of this work was to assess the sensitivity of GWPs to different agricultural practices in order to test mitigation options. The most efficient strategy we identified was to return crop residues to the soil, ie the wheat and barley straw. The worst one was to remove the organic fertiliser application which was a substantial input of C for the entire rotation. Although high CH_4 emissions were recorded immediately after application, they were stopped by soil incorporation a few hours later and the soil was a net sink of CH_4 during the rest of the year. The methane has little impact on the GHG balance but the incorporation of organic fertilisers immeditely after spreading appears as good option to reduce CH_4 emissions from organic fertilizer applications. In the same way, Jones et al. (2005) measured GHG fluxes from a managed grassland and reported that application of cattle slurry resulted in an immediate CH_4 peak flux of 2850 g CH_4-C ha^{-1} d^{-1}, during 2-3 days. However, CH_4 fluxes were insignificant compared to N_2O emissions in terme of GWP (1500 times lower).

Reducing N fertiliser rates lowers N_2O and indirect emissions of GHG, but also C fixation by plants. As a result, the fresh organic matter supply in soil from crop residues is diminished. For the Rafidin site, the most intensive system (N2) had the lowest GWP due to its large capacity

to store C fixed by crops. On the other hand, adding a third N fertiliser split application on the wheat crop in the rotation of the Grignon-PAN2 treatment resulted in a greater GWP due to higher indirect and N_2O emissions compared to the benefits in term of C fixation. This supplementary application was mostly aimed at increasing protein content and not plant biomass.

Assessing the effects of new mitigation strategies requires an integrated systems approach in order to encompass the indirect effects of mitigation strategies and counter-intuitive or unintentional flux changes (Robertson and Grace, 2004). Implementation of mitigation strategies that combines the options of i) enhancing soil carbon sequestration, ii) reducing N_2O emissions and iii) minimizing synthetic fertilizer use would be highly efficient in term of systemic reduction of GWP.

For example, Del Grosso et al. (2009) showed with the DAYCENT model that the most efficient strategy to reduce GHG fluxes, at the global scale, was to adopt no-till cultivation combined with nitrification inhibitors. However, no-till cultivation led to greater emissions in some wet regions of the world where soil moisture was conserved by no-till effect which enhanced denitrification and N_2O emissions which offseted the overall benefits of C storage.

Although the CERES-EGC model allowed us to quantify GWP of cropping systems and to test some mitigation strategies, it faced with a number of limitations, it lacks a capacity to i) well reproduce the effect of tillage practices on the soil C change, ii) reflect the nitrification inhibitor effects on N_2O emissions and iii) simulate methanogenesis and methanotrophy processes in soil and the resulting CH_4 fluxes. Further developments should focus on these points to improve the accuracy of GWP quantification and the assessment of mitigation options and new mitigation technologies.

5 Conclusion

The assessment of the direct emissions at the field scale is paramount in an accurate estimation of GHG balances for agricultural systems. Biophysical modelling of the soil-crop-atmosphere system provides a unique capacity to address this issue while taking into account the complex interactions between C and N cycling, as influenced by anthropogenic actions. Here, we tested and calibrated the CERES-EGC model to simulate the GHG fluxes of the agro-ecosystem, and showed it achieved satisfactory predictions of N_2O and CO_2 fluxes for different cropping systems representing distinct pedoclimatic conditions and agricultural practices.

The C dynamics predicted by the model were validated at the daily time scale against micrometeorological measurements of CO_2 exchanges in two of the three sites, but it will be necessary to supplement this test by further verifying the ability of CERES-EGC to simulate the rate of changes in the long term.

The modeling approach was used to devise different strategies to mitigate the GWP of cropping systems. Various scenarios involving some modifications of crop management (eg, fertilisation, rotation, crop residue management) were tested for this purpose. Other environmental impacts may be output by the model and included in the analysis, in particular the emissions into air or water of NH_3, NO_3^-, or NO. Thus, the overall environmental balance of the agricultural systems may be approached, making it possible to design agricultural systems with high environmental performance.

Acknowledgements

This work was part of the CarboEurope and NitroEurope Integrated Projects (EU's Sixth Framework Programme for Research and Technological Development), which both investigate the European terrestrial greenhouse gas balance. We express special thanks to Christophe Fléchard for

its assistance in the analysis of gas sampling.

References

Adler, P. R., Del Grosso, S. J., and Parton, W. J. (2007). Life-cycle assessment of net greenhouse-gas flux for bioenergy cropping systems. *Ecological Applications*, 17(3):675–691.

Adviento-Borbe, M. A. A., Haddix, M. L., Binder, D. L., Walters, D. T., and Dobermann, A. (2007). Soil greenhouse gas fluxes and global warming potential in four high-yielding maize systems. *Global Change Biology*, 13(9):1972–1988.

Ammann, C., Flechard, C. R., Leifeld, J., Neftel, A., and Fuhrer, J. (2007). The carbon budget of newly established temperate grassland depends on management intensity. *Agriculture, Ecosystems and Environment*, 121(1–2):5–20.

Anthoni, P. M., Knohl, A., Rebmann, C., Freibauer, A., Mund, M., Ziegler, W., Kolle, O., and Schulze, E. D. (2004). Forest and agricultural land-use-dependent CO2 exchange in thuringia, germany. *Global Change Biology*, 10(12):2005–2019.

Arrouays, D., Balesdent, J., Germon, J. C., Jayet, P. A., Soussana, J. F., and Stengel, P. (2002). *Stocker du carbone dans les sols agricoles de France?. Expertise scientifique collective*. INRA, Paris.

Aubinet, M., Grelle, A., Ibrom, A., Rannik, U., Moncrieff, J., Foken, T., Kowalski, A. S., Martin, P. H., Berbigier, P., Bernhofer, C., Clement, R., Elbers, J., Granier, A., Grunwald, T., Morgenstern, K., Pilegaard, K., Rebmann, C., Snijders, W., Valentini, R., and Vesala, T. (2000). Estimates of the annual net carbon and water exchange of forests: The EUROFLUX methodology. *Advances in Ecological Research*, 30:113–175.

Babu, Y. J., Li, C., Frolking, S., Nayak, D. R., and Adhya, T. K. (2006). Field validation of DNDC model for methane and nitrous oxide emissions from rice-based production systems of India. *Nutrient Cycling in Agroecosystems*, 74(2):157–174.

Bhatia, A., Pathak, H., Jain, N., Singh, P. K., and Singh, A. K. (2005). Global warming potential of manure amended soils under rice-wheat system in the Indo-Gangetic plains. *Atmospheric Environment*, 39(37):6976–6984.

Boote, K. J., Jones, J. W., and Pickering, N. B. (1996). Potential uses and limitations of crop models. *Agronomy Journal*, 88(5):704–716.

Conrad, R. (1996). Soil microorganisms as controllers of atmospheric trace gases (H2, CO, CH4, OCS, N2O, and NO). *Microbiological reviews*, 60(4):609–640.

Del Grosso, S. J., Halvorson, A., and Parton, W. (2008). Testing DAYCENT model simulations of corn yields and nitrous oxide emissions in irrigated tillage systems in Colorado. *Journal of Environmental Quality*, 37(4):1383–1389.

Del Grosso, S. J., Mosier, A. R., Parton, W. J., and Ojima, D. S. (2005). DAYCENT model analysis of past and contemporary soil N2O and net greenhouse gas flux for major crops in the USA. *Soil & Tillage Research*, 83(1):9–24.

Del Grosso, S. J., Ojima, D. S., Parton, W. J., Stehfest, E., Heistemann, M., DeAngelo, B., and Rose, S. (2009). Global scale DAYCENT model analysis of greenhouse gas emissions and mitigation strategies for cropped soils. *Global and Planetary Change*, In Press, Corrected Proof.

Desjardins, R. L., Smith, W., Grant, B., Campbell, C., and Riznek, R. (2005). Management strategies to sequester carbon in agricultural soils and to mitigate greenhouse gas emissions. *Climatic Change*, 70(1–2):283–297.

Falge, E., Baldocchi, D., Olson, R., Anthoni, P., Aubinet, M., Bernhofer, C., Burba, G., Ceulemans, G., Clement, R., Dolman, H., Granier, A., Gross, P., Grunwald, T., Hollinger, D., Jensen, N. O., Katul, G., Keronen, P., Kowalski, A., Lai, C. T., Law, B. E., Meyers, T., Moncrieff, J., Moors, E., Munger, J. W., Pilegaard, K., Rannik, U., Rebmann, C., Suyker, A., Tenhunen, J., Tu, K., Verma, S., Vesala, T., Wilson, K., and Wofsy, S. (2001). Gap filling strategies for long term energy flux data sets. *Agricultural and Forest Meteorology*, 107(1):71–77.

Frolking, S. E., Mosier, A. R., Ojima, D. S., Li, C., Parton, W. J., Potter, C. S., Priesack, E., Stenger, R., Haberbosch, C., Dorsch, P., Flessa, H., and Smith, K. A. (1998). Comparison of N_2O emissions from soils at three temperate agricultural sites: simulations of year-round measurements by four models. *Nutrient Cycling in Agroecosystems*, 52(2):77–105.

Gabrielle, B. and Gagnaire, N. (2008). Life-cycle assessment of straw use in bio-ethanol production: A case study based on biophysical modelling. *Biomass & Bioenergy*, 32(5):431–441.

Gabrielle, B., Laville, P., Duval, O., Nicoullaud, B., Germon, J. C., and Hénault, C. (2006). Process-based modeling of nitrous oxide emissions from wheat-cropped soils at the subregional scale. *Global Biogeochemical Cycles*, 20(4).

Gabrielle, B., Menasseri, S., and Houot, S. (1995). Analysis and field-evaluation of the CERES models water-balance component. *Soil Science Society of America journal*, 59(5):1403–1412.

Galloway, J. N., Townsend, A. R., Erisman, J. W., Bekunda, M., Cai, Z. C., Freney, J. R., Martinelli, L. A., Seitzinger, S. P., and Sutton, M. A. (2008). Transformation of the nitrogen cycle: Recent trends, questions, and potential solutions. *Science*, 320(5878):889–892.

Gelman, A. and Rubin, D. B. (1992). Inference from iterative simulation using multiple sequences. *Statistical Science*, 7(4):457–472.

Gijsman, A. J., Hoogenboom, G., Parton, W. J., and Kerridge, P. C. (2002). Modifying DSSAT crop models for low-input agricultural systems using a soil organic matter-residue module from CENTURY. *Agronomy Journal*, 94(3):462–474.

Gosse, G., Cellier, P., Denoroy, P., Gabrielle, B., Laville, P., Leviel, B., Justes, E., Nicolardot, B., Mary, B., Recous, S., Germon, J. C., Hénault, C., and Leech, P. K. (1999). Water, carbon and nitrogen cycling in a rendzina soil cropped with winter oilseed rape: the chalons oilseed rape database. *Agronomie*, 19(2):119–124.

Grace, P. R., Jain, M. C., Harrington, L. W., and Robertson, G. P. (1993). Long-term sustainability of the tropical and subtropical rice and wheat system: An environmental perspective. In Ladha, J. K., Hill, J. E., Duxbury, J. M., Gupta, R. K., and Buresh, R. J., editors, *Improving the Productivity and Sustainability of Rice-Wheat System: Issues and Impacts*, pages 27–43. ASA Special publication 65.

Grant, R. F., Arkebauer, T. J., Dobermann, A., Hubbard, K. G., Schimelfenig, T. T., Suyker, A. E., Verma, S. B., and Walters, D. T. (2007). Net Biome Productivity of Irrigated and Rainfed Maize Soybean Rotations: Modeling vs. Measurements. *Agronomy Journal*, 99(6):1404–1423.

Hénault, C., Bizouard, F., Laville, P., Gabrielle, B., Nicoullaud, B., Germon, J. C., and Cellier, P. (2005). Predicting in situ soil n2o emission using NOE algorithm and soil database. *Global Change Biology*, 11(1):115–127.

Hénault, C. and Germon, J. C. (2000). NEMIS, a predictive model of denitrification on the field scale. *European Journal of Soil Science*, 51(2):257–270.

Hutchinson, G. L. and Davidson, E. A. (1993). Processes for Production and Consumption of Gaseous Nitrogen Oxides in Soil. In Rolston, D., Duxbury, J., Harper, L., and Mosier, A.,

editors, *Agricultural Ecosystem Effects on trace Gases and Global Climate Change*, chapter 5. ASA Special publication 55.

IPCC (2007). *Climate Change 2007 - The Physical Science Basis: Working Group I Contribution to the Fourth Assessment Report of the IPCC (Climate Change 2007)*. Cambridge University Press.

Jones, C. A. and Kiniry, J. R. (1986). *CERES-N Maize: a simulation model of maize growth and development*. Texas A&M University Press, College Statio, Temple, TX.

Jones, S. K., Rees, R. M., Skiba, U. M., and Ball, B. C. (2005). Greenhouse gas emissions from a managed grassland. *Global and Planetary Change*, 47(2–4):201–211.

Jungkunst, H. F., Freibauer, A., Neufeldt, H., and Bareth, G. (2006). Nitrous oxide emissions from agricultural land use in Germany - a synthesis of available annual field data. *Journal of Plant Nutrition and Soil Science-zeitschrift Fur Pflanzenernahrung Und Bodenkunde*, 169(3):341–351.

Kaiser, E. A. and Ruser, R. (2000). Nitrous oxide emissions from arable soils in Germany - An evaluation of six long-term field experiments. *Journal of Plant Nutrition and Soil Science-zeitschrift Fur Pflanzenernahrung Und Bodenkunde*, 163(3):249–259.

Kim, S. and Dale, B. E. (2005). Environmental aspects of ethanol derived from no-tilled corn grain: nonrenewable energy consumption and greenhouse gas emissions. *Biomass & Bioenergy*, 28(5):475–489.

Lamboni, M., Makowski, D., Lehuger, S., Gabrielle, B., and Monod, H. (2009). Multivariate global sensitivity analysis for dynamic crop model. *Field crop Research*, In Submission.

Lehuger, S., Gabrielle, B., Van Oijen, M., Makowski, D., Germon, J. C., Morvan, T., and Hénault, C. (2009). Bayesian calibration of the nitrous oxide emission module of an agro-ecosystem model. agriculture, ecosystem and environment. *Agriculture, Ecosystems and Environment*, In Press.

Li, C. S., Frolking, S., and Butterbach-Bahl, K. (2005a). Carbon sequestration in arable soils is likely to increase nitrous oxide emissions, offsetting reductions in climate radiative forcing. *Climatic Change*, 72(3):321–338.

Li, C. S., Frolking, S., and Frolking, T. A. (1992). A Model of Nitrous-oxide Evolution From Soil Driven by Rainfall Events .1. Model Structure and Sensitivity. *Journal of Geophysical Research-atmospheres*, 97(9):9759–9776.

Li, Y., Chen, D. L., Zhang, Y. M., Edis, R., and Ding, H. (2005b). Comparison of three modeling approaches for simulating denitrification and nitrous oxide emissions from loam-textured arable soils. *Global Biogeochemical Cycles*, 19(3).

Makowski, D., Hillier, J., Wallach, D., Andrieu, B., and Jeuffroy, M. H. (2006). Parameter estimation for crop models. In Wallach, D., Makowski, D., and Jones, J. W., editors, *Working with dynamic crop models: evaluating, analyzing, parameterizing and using them*, chapter 4. Elsevier.

Metropolis, N., Rosenbluth, A. W., Rosenbluth, M. N., Teller, A. H., and Teller, E. (1953). Equation of state calculations by fast computing machines. *Journal of Chemical Physics*, 21(6):1087–1092.

Mosier, A. R., Halvorson, A. D., Peterson, G. A., Robertson, G. P., and Sherrod, L. (2005). Measurement of net global warming potential in three agroecosystems. *Nutrient Cycling in Agroecosystems*, 72(1):67–76.

Nemecek, T., Heil, A., Huguenin, O., Erzinger, S., Blaser, S., Dux, D., and Zimmerman, A. (2003). *Life Cycle Inventories of Production Systems. Final report Ecoinvent 2000, No 15*. FAL Reckenholz, FAT Tanikon, Swiss Centre For Life Cycle Inventories, Dubendorf, CH.

Pathak, H., Li, C., and Wassmann, R. (2005). Greenhouse gas emissions from Indian rice fields: calibration and upscaling using the DNDC model. *Biogeosciences*, 2(2):113–123.

Robertson, G. P. and Grace, P. R. (2004). Greenhouse gas fluxes in tropical and temperate agriculture: The need for a full-cost accounting of global warming potentials. *Environment, Development and Sustainability*, 6:51–63.

Robertson, G. P., Paul, E. A., and Harwood, R. R. (2000). Greenhouse gases in intensive agriculture: Contributions of individual gases to the radiative forcing of the atmosphere. *Science*, 289(5486):1922–1925.

Six, J., Ogle, S. M., Breidt, F. J., Conant, R. T., Mosier, A. R., and Paustian, K. (2004). The potential to mitigate global warming with no-tillage management is only realized when practised in the long term. *Global Change Biology*, 10(2):155–160.

Smith, P., Goulding, K. W., Smith, K. A., Powlson, D. S., Smith, J. U., Falloon, P., and Coleman, K. (2001). Enhancing the carbon sink in European agricultural soils: including trace gas fluxes in estimates of carbon mitigation potential. *Nutrient Cycling in Agroecosystems*, 60(1–3):237–252.

Smith, P., Martino, D., Cai, Z., Gwary, D., Janzen, H., Kumar, P., McCarl, B., Ogle, S., OMara, F., Rice, C., Scholes, B., and Sirotenko, O. (2007). *Agriculture. In Climate Change 2007: Mitigation. Contribution of Working Group III to the Fourth Assessment Report of the Intergovernmental Panel on Climate Change, [B. Metz, O.R. Davidson, P.R. Bosch, R. Dave, L.A.*

Meyer (eds)]. Cambridge University Press, Cambridge, United Kingdom and New York, NY, USA.

Sutton, M. A., Nemitz, E., Erisman, J. W., Beier, C., Bahl, K. B., Cellier, P., de Vries, W., Cotrufo, F., Skiba, U., Di Marco, C., Jones, S., Laville, P., Soussana, J. F., Loubet, B., Twigg, M., Famulari, D., Whitehead, J., Gallagher, M. W., Neftel, A., Flechard, C. R., Herrmann, B., Calanca, P. L., Schjoerring, J. K., Daemmgen, U., Horvath, L., Tang, Y. S., Emmett, B. A., Tietema, A., Penuelas, J., Kesik, M., Brueggemann, N., Pilegaard, K., Vesala, T., Campbell, C. L., Olesen, J. E., Dragosits, U., Theobald, M. R., Levy, P., Mobbs, D. C., Milne, R., Viovy, N., Vuichard, N., Smith, J. U., Smith, P., Bergamaschi, P., Fowler, D., and Reis, S. (2007). Challenges in quantifying biosphere-atmosphere exchange of nitrogen species. *Environmental Pollution*, 150(1):125–139.

Trinsoutrot, I., Nicolardot, B., Justes, E., and Recous, S. (2000). Decomposition in the field of residues of oilseed rape grown at two levels of nitrogen fertilisation. Effects on the dynamics of soil mineral nitrogen between successive crops. *Nutrient Cycling in Agroecosystems*, 56(2):125–137.

Van Oijen, M., Rougier, J., and Smith, R. (2005). Bayesian calibration of process-based forest models: bridging the gap between models and data. *Tree Physiology*, 25(7):915–927.

Wallach, D. (2006). Evaluating crop models. In Wallach, D., Makowski, D., and Jones, J. W., editors, *Working with dynamic crop models: evaluating, analyzing, parameterizing and using them*, chapter 2. Elsevier.

West, T. O. and Marland, G. (2002). Net carbon flux from agricultural ecosystems: methodology for full carbon cycle analyses. *Environmental Pollution*, 116(3):439–444.

Zhang, Y., Li, C., Zhou, X., and Moore, B. (2002). A simulation model linking crop growth and soil biogeochemistry for sustainable agriculture. *Ecological Modelling*, 151(1):75–108.

List of Tables

Site	Crop	Sowing date	N Fertilizer	
			Date	Amount (kg N ha^{-1})
GRIGNON-PP	Wheat	16/10/2002	26/02/2003	52
			27/03/2003	60
	Barley	17/10/2003	18/02/2004	59
			19/03/2004	59
			02/04/2004	39
	Mustard	02/09/2004	31/08/2004	Slurry (90)
	Maize	09/05/2005	09/05/2005	140
	Wheat	16/10/2005	15/03/2006	55
			14/04/2006	55
	Barley	06/10/2006	22/02/2007	55
			22/03/2007	55
	Mustard	22/09/2007	17/04/2008	Slurry (80)
	Maize	28/04/2008	05/05/2008	60
RAFIDIN	Rapeseed N0	09/04/1994		
	Rapeseed N1	09/04/1994	20/02/1995	80
			15/03/1995	75
	Rapeseed N2	09/04/1994	12/09/1994	49
			20/02/1995	80
			15/03/1995	75
			29/03/1995	38
	Wheat	27/10/1995	10/02/1996	60
			10/03/1996	95
			10/05/1996	65
	Barley	27/10/1995	10/02/1997	90
			10/03/1997	80
GRIGNON-PAN1	Wheat	27/10/2005	06/03/2006	50
			07/04/2006	110
	Barley	06/10/2006	04/03/2007	50
			26/03/2007	70
	Mustard	31/08/2007		
	Maize	07/05/2008	08/05/2008	140
GRIGNON-PAN2	Barley	05/10/2005	06/03/2006	50
			07/04/2006	50
	Mustard	30/09/2006		
	Maize	26/04/2007	02/05/2007	150
	Wheat	24/10/2007	14/02/2008	50
			03/04/2008	120
			15/05/2008	40
GRIGNON-PAN3	Mustard	02/09/2005		
	Maize	26/04/2006	04/05/2006	160
	Wheat	10/10/2006	05/03/2007	50
			26/03/2007	70
	Barley	08/10/2007	15/02/2008	50
			05/04/2008	90
GEBESEE	Sugar beet	20/10/2006	10/04/2006	30
	Wheat	27/10/2006	27/03/2007	80
			11/04/2007	Slurry (20)
			03/05/2007	85
			03/09/2007	FYM (200)

Table 3: Experimental treatments and N input rates at the Grignon, Rafidin and Gebesee sites.

Site	Treatment	RMSE or RMSEP (in italics) computed with:	
		Initial parameter values	Posterior expectancy of parameters
Grignon-PP		20.2	14.2
Rafidin	N0	4.6	0.3
	N1	10.4	1.4
	N2	15.9	3.0
Grignon-PAN1		10.4	*9.6*
Grignon-PAN2		7.4	*7.0*
Grignon-PAN3		7.6	*7.3*
Gebesee		7.6	*4.6*

Table 4: Root mean square errors (RMSEs) of daily nitrous oxide emissions, based on the initial parameters values and the posterior expectancy of parameters. The posterior expectancy of parameters was computed from the the Bayesian calibration of the nitrous oxide module of CERES-EGC against the N_2O measurements of the Rafidin site and of the Grignon-PP experimental site. For the Grignon-PAN1, -PAN2, -PAN3 and the Gebesee sites, the RMSEP was computed with the posterior expectancy of parameters based on the Bayesian calibration against the N_2O measurements of the Grignon-PP site.

	Time period		CO_2	N_2O	CH_4	Agricultural inputs	Net GWP
	Start	End	kg CO_2-C eq ha^{-1}				
GRIGNON-PP							
Maize	9 May n	15 Oct. n	27(4)	179(45)	-2	310	514(55)
Wheat	16 Oct. n	5 Oct. n+1	969(139)	235(66)	-5	324	1522(204)
Barley	6 Oct. n+1	21 Oct. n+2	356(45)	400 (94)	-5	338	1087(138)
Mustard	22 Oct. n+2	8 May n+3	-1322(68)	136(41)	3	70	-1112(55)
Rotation	9 May n	8 May n+3	29(255)	949(247)	-9	1042	2011(453)
RAFIDIN							
Rapeseed N0	10 Sept. n	26 Oct. n+1	187(144)	101(18)	-	99	387(162)
Wheat	27 Oct n+1	26 Oct n+2	-1701(473)	128(41)	-	471	-1102(246)
Barley	27 Oct n+2	9 Sept. n+3	-61(12)	108(43)	-	397	444(43)
Rotation N0	10 Sept. n	9 Sept. n+3	-1575(629)	338(101)	-	967	-270(451)
Rapeseed N1	10 Sept. n	26 Oct. n+1	-1850(348)	121(27)	-	359	-1370(220)
Wheat	27 Oct n+1	26 Oct n+2	-1355(361)	135(44)	-	471	-750(155)
Barley	27 Oct n+2	9 Sept. n+3	-255(47)	117(44)	-	397	258(31)
Rotation N1	10 Sept. n	9 Sept. n+3	-3460(756)	372(114)	-	1226	-1862(406)
Rapeseed N2	10 Sept. n	26 Oct. n+1	-2158(429)	159(28)	-	506	-1493(241)
Wheat	27 Oct n+1	26 Oct n+2	-1339(354)	136(45)	-	471	-732(150)
Barley	27 Oct n+2	9 Sept. n+3	-309(58)	119(44)	-	397	206(25)
Rotation N2	10 Sept. n	9 Sept. n+3	-3806(841)	414(116)	-	1374	-2019(417)

Table 5: Predictions of net global warming potential (GWP) from simulations of net biome production (CO_2=-NBP) and N_2O emissions, estimation of methane fluxes from chamber measurements and indirect GHG costs of agricultural inputs. Simulations were averaged over 36 and 28 years for Grignon-PP and Rafidin cropping systems, resp.

	Time period		CO_2	N_2O	CH_4	Agricultural inputs	Net GWP
	Start	End	kg CO_2-C eq ha^{-1}				
GRIGNON-PAN1							
Wheat	27/10/05	05/10/06	1587	117	-6	371	2070
Barley	06/10/06	30/08/07	-209	208	-5	475	469
Mustard	31/08/07	06/05/08	579	101	-4	109	784
Maize	07/05/08	26/10/08	-2211	119	-3	299	-1796
Rotation	27/10/05	26/10/08	-254	545	-18	1253	1526
GRIGNON-PAN2							
Barley	05/10/05	29/09/06	548	154	-13	224	913
Mustard	30/09/06	25/04/07	537	164	-8	115	808
Maize	26/04/07	23/10/07	-2310	140	-7	448	-1729
Wheat	24/10/07	04/10/08	1994	123	-13	643	2747
Rotation	05/10/05	04/10/08	769	580	-40	1430	2739
GRIGNON-PAN3							
Mustard	02/09/05	25/04/06	372	71	-3	45	485
Maize	26/04/06	09/10/06	-2592	80	-2	241	-2274
Wheat	10/10/06	07/10/07	2023	221	-4	455	2695
Barley	08/10/07	01/09/08	101	139	-4	497	734
Rotation	02/09/05	01/09/08	-97	511	-12	1238	1640
GEBESEE							
Wheat	27/10/06	05/10/07	-3773	158	-4	589	-3030

Table 6: Predictions of net global warming potential (GWP) from simulations of net biome production (CO_2=-NBP) and N_2O emissions, estimation of methane fluxes from chamber measurements and indirect GHG costs of agricultural inputs, for the one-year wheat crop cycle of Gebesee and the three treatments PAN1, PAN2 and PAN3 of Grignon.

List of Figures

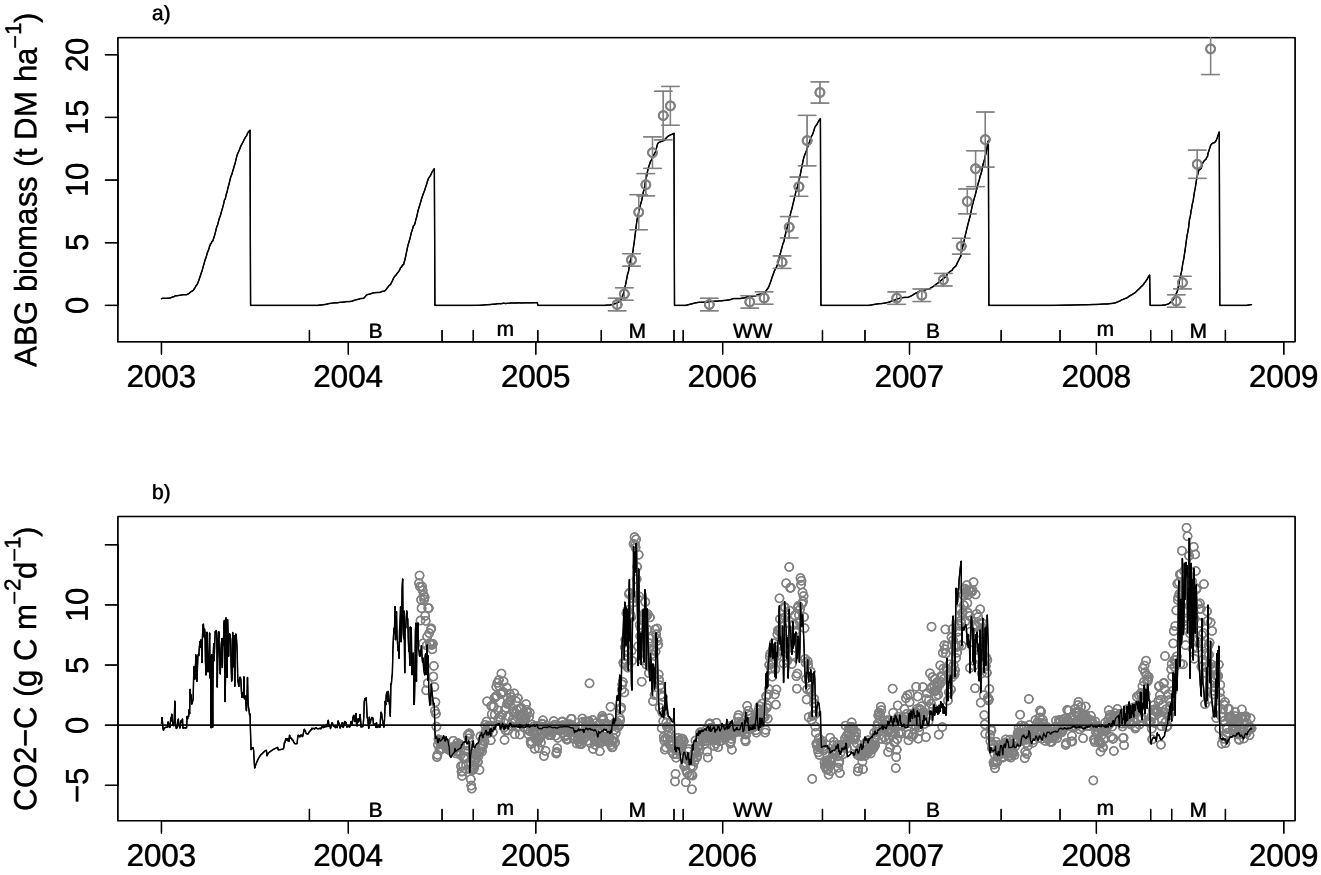

Figure 1: Simulations (black line) and observations (grey points) of above-ground (ABG) crop biomass (a) and times course of simulated (black line) and observed (grey symbols) of net ecosystem production (NEP) on a daily time scale (b), at the Grignon-PP experimental field.

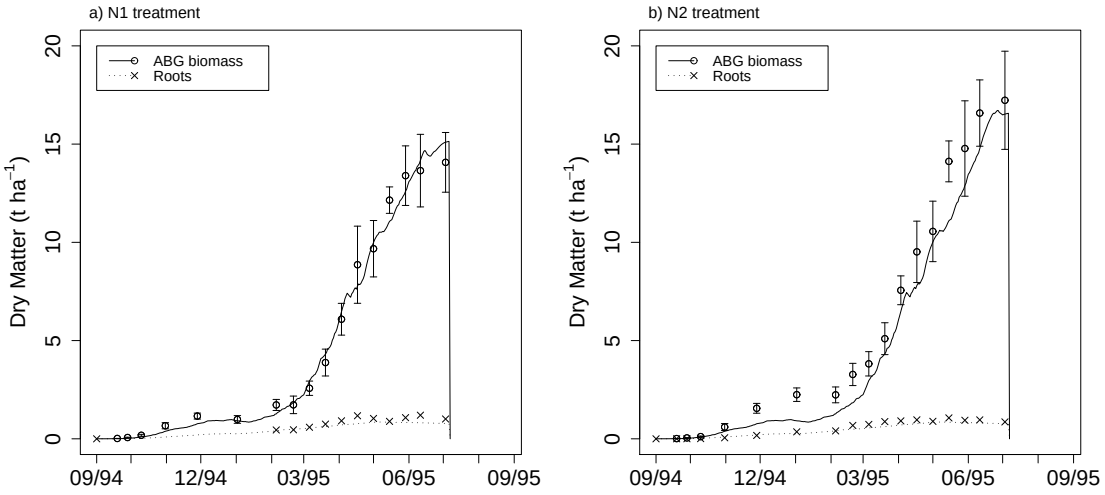

Figure 2: Simulated (lines) and measured (symbols $\pm$ sd) data for (a) above ground (ABG) dry matter and roots for N1 treatment, (b) above ground (ABG) dry matter and roots for N2 treatment, in 1995 at Rafidin (France).

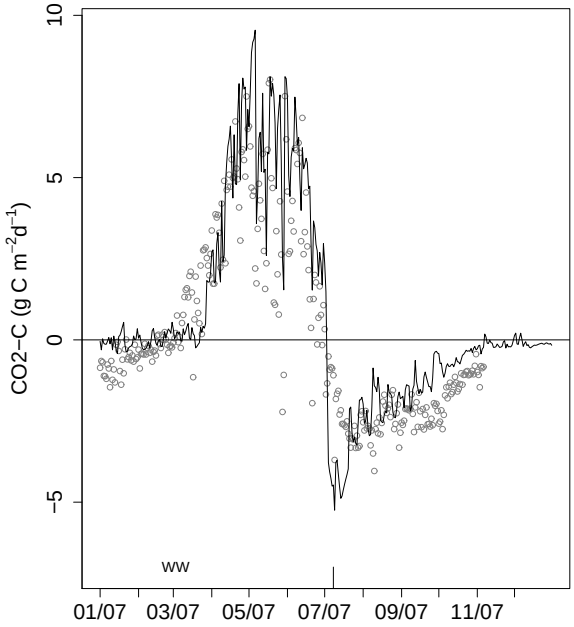

Figure 3: Simulated (black line) and observed (grey points) of daily net ecosystem production (NEP) for the wheat crop cycle of Gebesee.

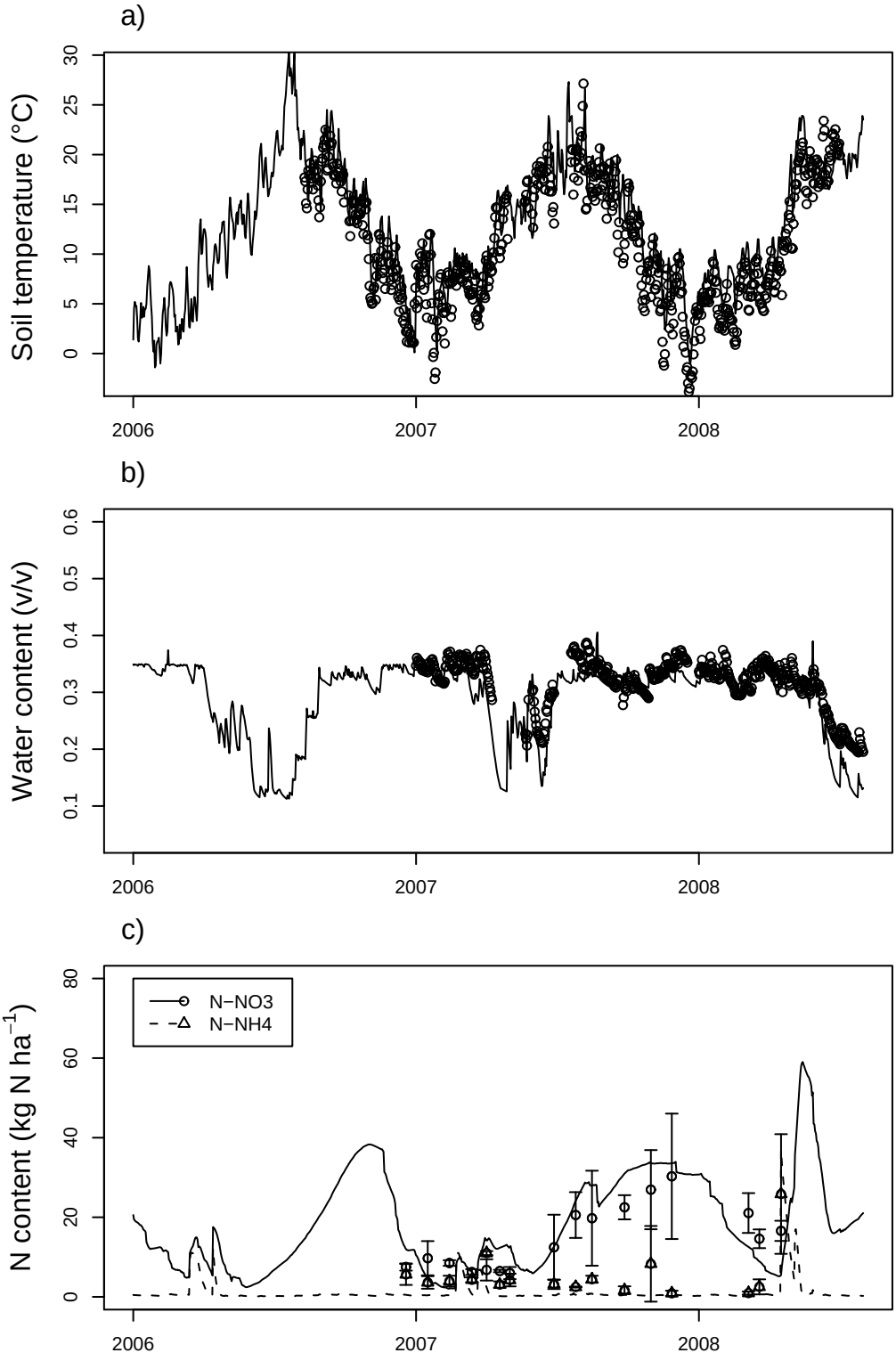

Figure 4: Simulated (line) and observed (symbols $\pm sd$) of daily soil temperature (a), soil water content (b) and nitrogen content in the 0-15 cm topsoil layer (c), for the experimental field site of Grignon-PP.

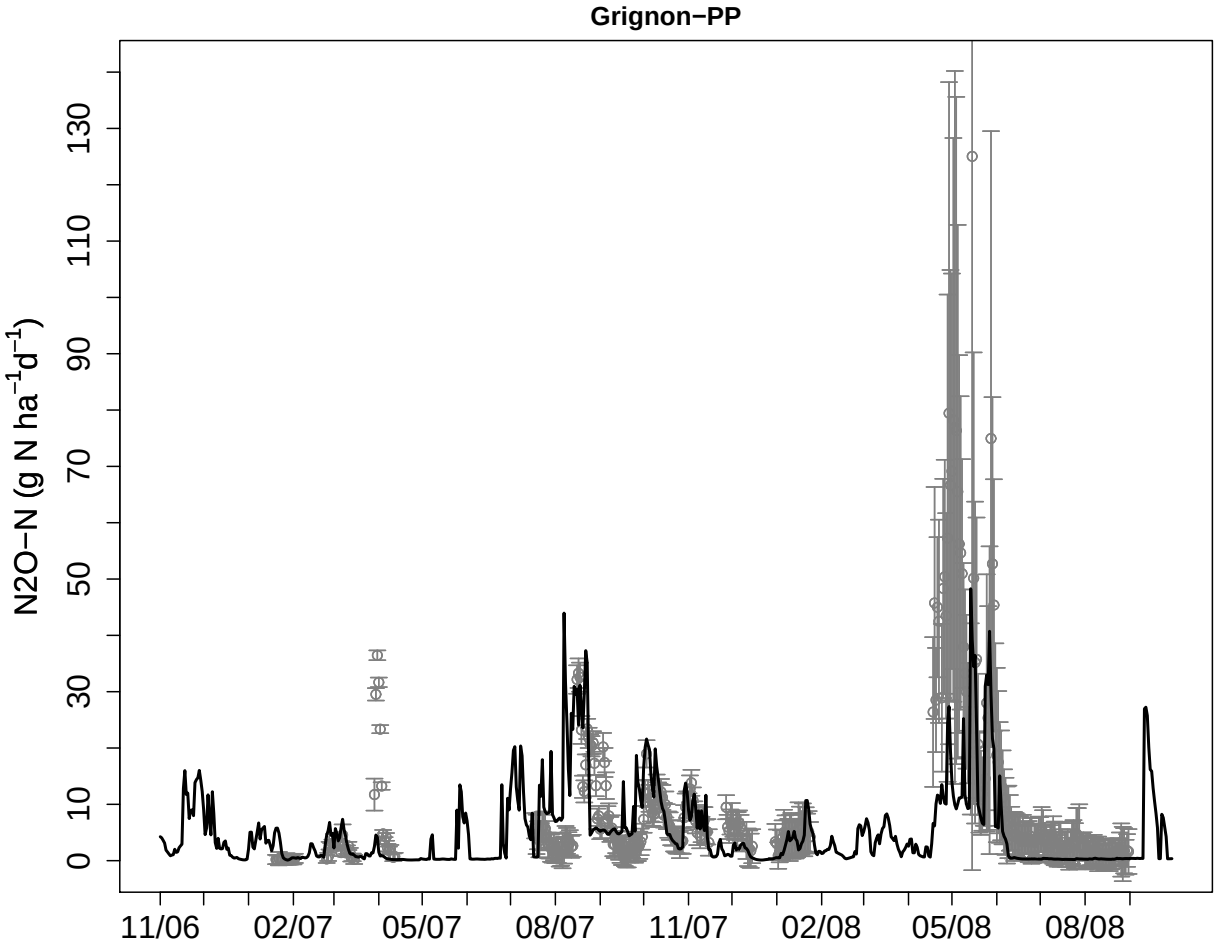

Figure 5: Simulated (black line) and observed (symbols $\pm sd$) of daily nitrous oxide emissions for the Grignon-PP experimental site.

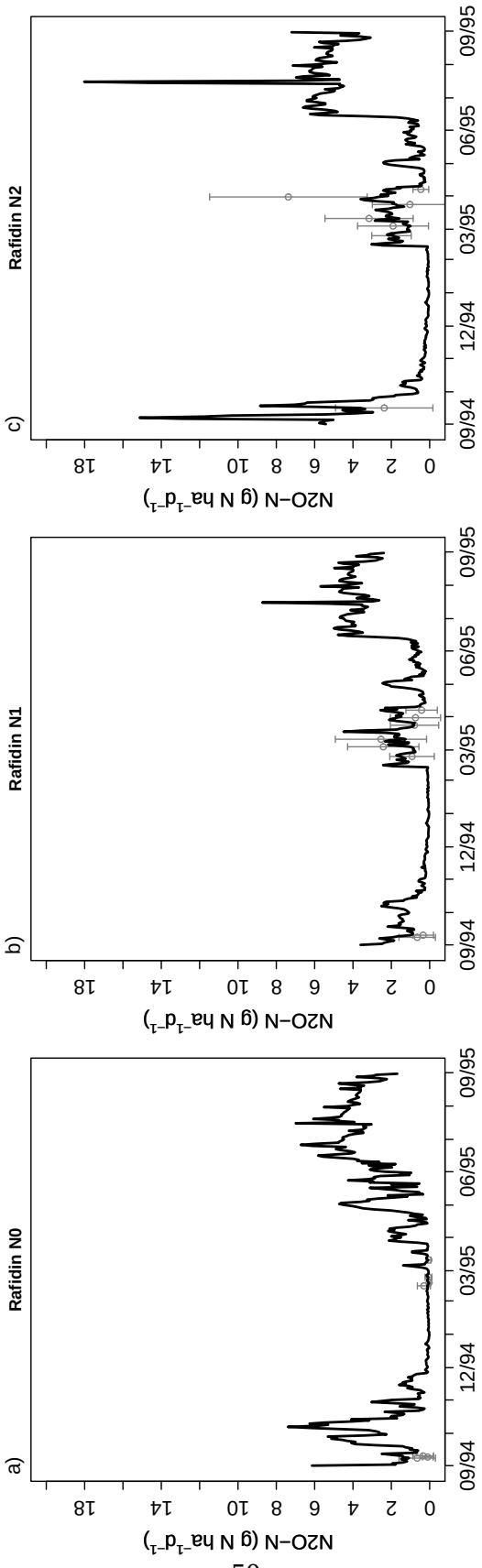

Figure 6: Simulated (line) and observed (symbols $\pm sd$) of daily nitrous oxide emissions for the N0 (a), N1 (b) and N2 treatment (c) of the Rafidin experimental site.

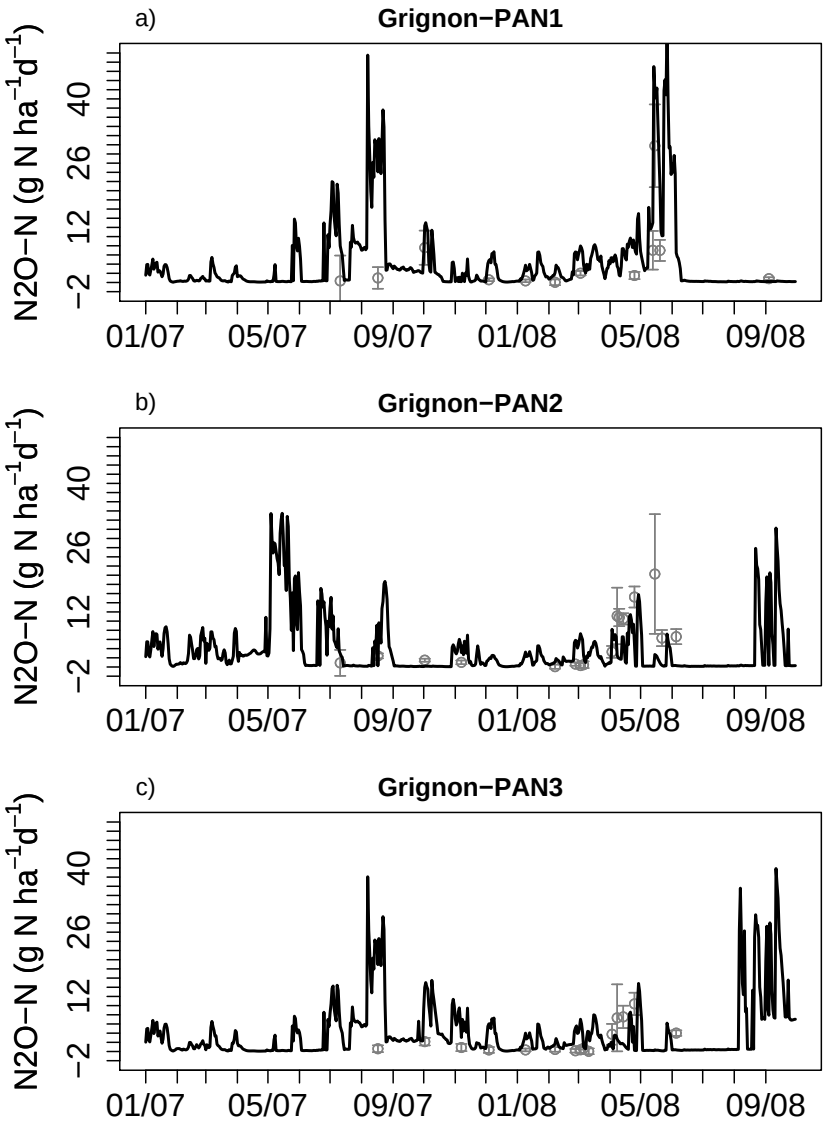

Figure 7: Simulated (line) and observed (symbols $\pm sd$) of daily nitrous oxide emissions for the Grignon-PAN1 (a), -PAN2 (b) and -PAN3 (c) experiments.

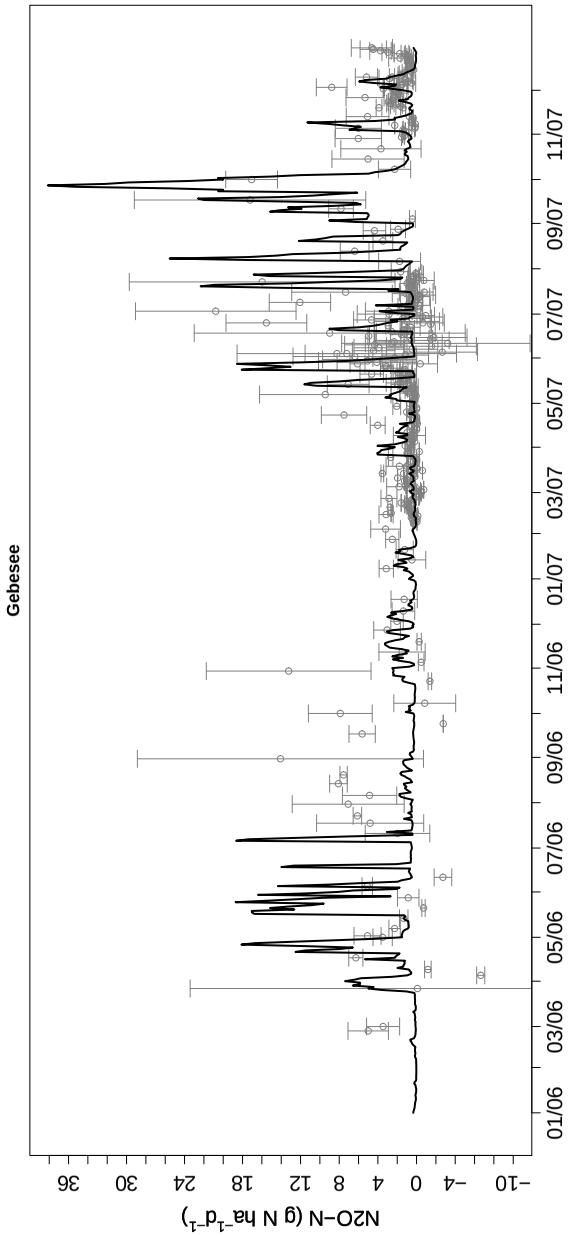

Figure 8: Simulated (line) and observed (symbols $\pm sd$) of daily nitrous oxide emissions for the Gebesee experimental field sites.

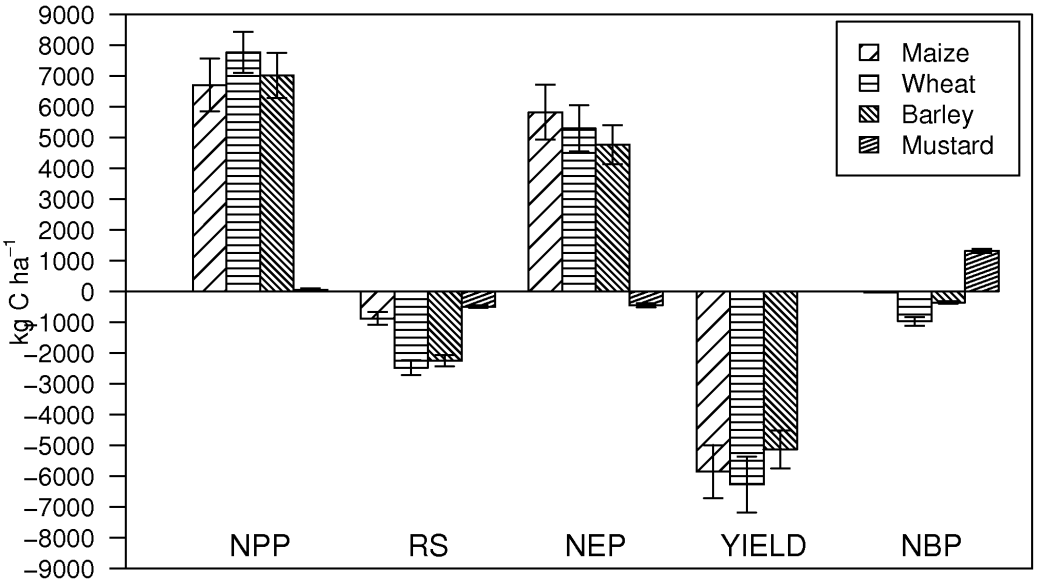

Figure 9: Breakdown of net biome production (NBP) into net primary production (NPP), soil respiration (Rs), net ecosystem production (NEP), grain or silage yields plus straw removal (YIELD) for the four crops of the rotation (maize, wheat, barley, mustard) at the Grignon-PP experimental site.

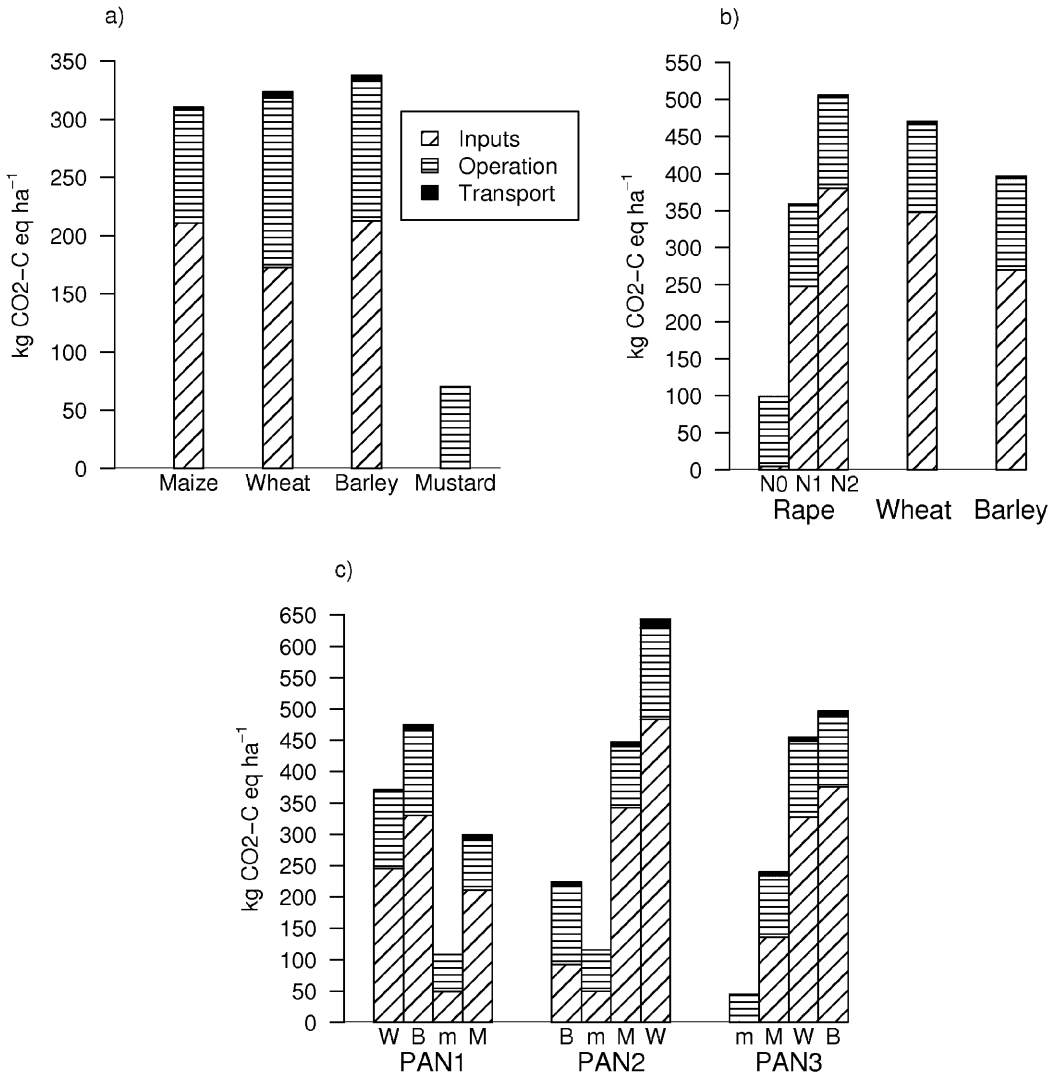

Figure 10: Greenhouse gas cost of agricultural inputs and cropping operations for crop production (indirect emissions) for the Grignon-PP (a), Rafidin (b) and Grignon-PANs (c) cropping systems. The emissions are broken down into the input production, agricultural operations and transport steps.

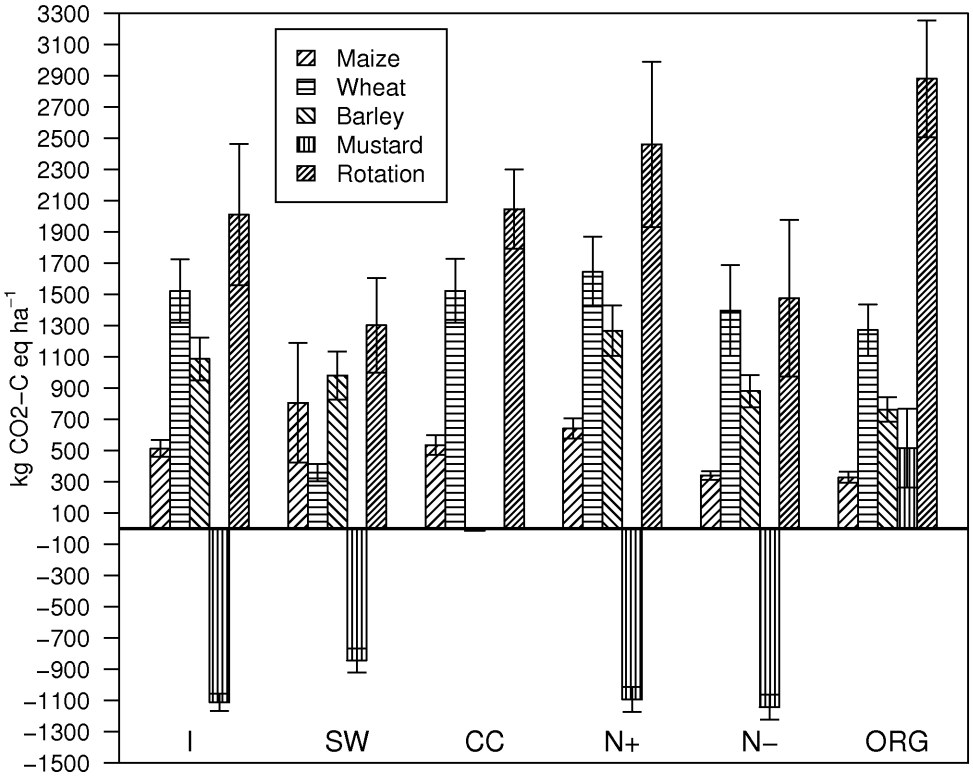

Figure 11: Comparison of net global warming potentials of five scenarios averaged over 36-years for the Grignon-PP experiment (I: initial scenario, SW: straw left on soil, CC: without catch crop, N+: 50% more N fertiliser, N-: 50% less N fertiliser, ORG: without organic fertiliser).